CONFIDENTIAL
RESTRICTED

COPY NO. 81
RM No. E8F10c

222A

C1

NACA

RESEARCH MEMORANDUM

PRELIMINARY RESULTS OF AN ALTITUDE-WIND-TUNNEL INVESTIGATION OF AN AXIAL-FLOW GAS TURBINE-PROPELLER ENGINE

IV - COMPRESSOR AND TURBINE PERFORMANCE CHARACTERISTICS

By Lewis E. Wallner and Martin J. Saari

Flight Propulsion Research Laboratory
Cleveland, Ohio

CLASSIFICATION CHANGED

To Confidential
EO-10501 NACA RF 1730

By authority of J W Crowley
JH 1/15/54

CLASSIFIED DOCUMENT

This document contains classified information affecting the National Defense of the United States within the meaning of the Espionage Act, USC 50:31 and 32. Its transmission or the revelation of its contents in any manner to an unauthorized person is prohibited by law. Information so classified may be imparted only to persons in the military and naval services of the United States, appropriate civilian officers and employees of the Federal Government who have a legitimate interest therein, and to United States citizens of known loyalty and discretion who of necessity must be informed thereof.

CLASSIFICATION CANCELLED
& Unclassified
Authority NACA Res. Abs. Date 9-20-56
& RN-104
By NB 8-6-56 See

TECHNICAL EDITING WAIVED

NATIONAL ADVISORY COMMITTEE FOR AERONAUTICS

WASHINGTON
August 10, 1948

RESTRICTED
CONFIDENTIAL

[redacted]

 [redacted]

NASA Technical Library
3 1176 01435 5409

NATIONAL ADVISORY COMMITTEE FOR AERONAUTICS

RESEARCH MEMORANDUM

PRELIMINARY RESULTS OF AN ALTITUDE-WIND-TUNNEL INVESTIGATION OF AN AXIAL-FLOW GAS TURBINE-PROPELLER ENGINE

IV - COMPRESSOR AND TURBINE PERFORMANCE CHARACTERISTICS

By Lewis E. Wallner and Martin J. Saari

SUMMARY

As part of an investigation of the performance and operational characteristics of the axial-flow gas turbine-propeller engine, conducted in the Cleveland altitude wind tunnel, the performance characteristics of the compressor and the turbine were obtained. The data presented were obtained at a compressor-inlet ram-pressure ratio of 1.00 for altitudes from 5000 to 35,000 feet, engine speeds from 8000 to 13,000 rpm, and turbine-inlet temperatures from 1400° to 2100° R.

The highest compressor pressure ratio obtained was 6.15 at a corrected air flow of 23.7 pounds per second and a corrected turbine-inlet temperature of 2475° R. Peak adiabatic compressor efficiencies of about 77 percent were obtained near the value of corrected air flow corresponding to a corrected engine speed of 13,000 rpm. This maximum efficiency may be somewhat low, however, because of dirt accumulations on the compressor blades.

A maximum adiabatic turbine efficiency of 81.5 percent was obtained at rated engine speed for all altitudes and turbine-inlet temperatures investigated.

INTRODUCTION

An investigation of the performance and operational characteristics of an axial-flow gas turbine-propeller engine has been

[redacted]

[redacted]

conducted in the Cleveland altitude wind tunnel. Engine performance characteristics, windmilling characteristics, and pressure and temperature distributions throughout the engine are presented in references 1, 2, and 3, respectively.

The performance of the compressor and the turbine are of particular significance because very little altitude data have been obtained on these component parts in a gas turbine-propeller engine. Data were obtained at a compressor-inlet ram-pressure ratio of 1.00 at altitudes from 5000 to 35,000 feet, engine speeds from 8000 to 13,000 rpm, and turbine-inlet temperatures from 1400° to 2100° R. The compressor performance is presented as a function of corrected engine air flow and corrected turbine-inlet temperature. The turbine performance is presented as a function of corrected turbine speed and corrected turbine-inlet temperature.

DESCRIPTION OF COMPRESSOR AND TURBINE

A general description of the T31 gas turbine-propeller engine and the installation is given in reference 1. A detailed description of the compressor and turbine assemblies is given in the following sections.

Compressor

The T31 engine is equipped with a 14-stage axial-flow compressor, which has a sea-level air-flow rating of about 21 pounds per second at an engine speed of 13,000 rpm. The compressor rotor, shown in figure 1, consists of 14 wheels shrunk on a hollow shaft. The compressor blades are dovetailed into the rotor wheels. The blade-tip diameter of the rotor is $16\frac{9}{16}$ inches and the over-all length is 25 inches. The hub-to-tip diameter ratio at the first rotor stage is 0.73 and increases to 0.88 at the fourteenth rotor stage. A balance pressure is applied to the forward end of the rotor by air bled from the fifth stage of the compressor. This air leaks out through two labyrinth seals into the compressor air passage aft of the inlet guide vanes. Another labyrinth seal is located at the aft end of the rotor. Air leaking through this seal is used to cool the forward face of the turbine wheel.

The stator stages consist of half rings into which the stator blades are dovetailed (fig. 2). These half rings, assembled around the rotor with spacers and clamping bolts, compose the compressor stator assembly.

Air enters the compressor through an annular inlet, which is divided into six equal segments by radial support struts. The flow area of the compressor inlet (station 2, fig. 3) is approximately 95 square inches. A single row of guide vanes turns the air in the direction of rotation of the rotor. Air is discharged from the compressor through two rows of straightening vanes into an annular passage.

Turbine Assembly

The T31 engine has a single-stage turbine that delivers about 5000 horsepower at standard sea-level conditions and an engine speed of 13,000 rpm. The turbine (fig. 4) has a solid steel disk that tapers in thickness from 3.70 inches at the hub to 0.57 inch at the thinnest section near the rim. The turbine blades, which are welded to the wheel rim, are 1.6 inches in length. The blade chord tapers from 1.0 inch at the root to 0.75 inch at the tip. The blade forgings are so designed that the rectangular tips in the assembled wheel form the turbine shroud ring. The over-all diameter of the wheel including the shroud ring is 28 inches. The turbine clearances are shown in the detail of figure 3.

The turbine nozzle (fig. 5), which consists of 36 equally spaced hollow steel vanes, has an actual flow area of about 25 square inches and an expansion ratio of 1.065. The vanes are welded to inner and outer shroud rings. A portion of the air that enters the combustion chambers first flows through the hollow vanes to provide cooling.

Gases discharged from the turbine enter an annular exhaust cone having an area of about 154 square inches at the location of the turbine-outlet instrumentation (station 6, fig. 3). The inner cone is supported by four struts and by a series of small angle braces extending along the entire length of the inner cone. In the wind-tunnel investigation, a straight tail pipe 14 inches in diameter and 96 inches long was used.

INSTRUMENTATION

A complete description of the instrumentation throughout the installation is given in reference 1. A review of the instrumentation required to determine the compressor and turbine characteristics is presented herein.

The annular compressor inlet was divided into six equal segments by the radial support struts, which form part of the engine structure. Installed in each alternate segment were five total-pressure tubes, two iron-constantan thermocouples, two static-pressure probes, and a static-pressure wall orifice on the inner and outer walls of the annulus. The remaining three segments had only static-pressure wall orifices installed on the outer walls. (See fig. 6.) Installed at the compressor outlet were nine total-pressure tubes, six iron-constantan thermocouples, two static-pressure probes, and five static-pressure wall orifices (fig. 7).

The turbine inlet was instrumented with five total-pressure tubes and five static-pressure wall orifices. Three of the total-pressure tubes were located 120° apart. One of the areas included by a single burner transition section had two additional total-pressure tubes installed 10° on each side of the center tube (fig. 8). The turbine outlet, or exhaust-cone inlet, was instrumented with three rakes, 120° apart, each containing three total-pressure tubes. A static-pressure wall orifice was installed on the outer wall in the plane of each rake. Three wafer static tubes were installed at various immersions and were rotated 20° from each of the total-pressure rakes. A chromel-alumel thermocouple was installed approximately in line with the center of each of the nine combustion chambers to indicate combustion-chamber ignition and unbalance (fig. 9).

Exhaust-gas temperatures were measured with six chromel-alumel thermocouples at the tail-pipe-nozzle outlet (fig. 10).

PROCEDURE

Data were obtained at a compressor-inlet ram-pressure ratio of 1.00, pressure altitudes from 5000 to 35,000 feet, and engine speeds from 8000 to 13,000 rpm. Ambient temperatures were maintained at approximately NACA standard altitude conditions. The engine power was varied to give turbine-inlet temperatures ranging from 1400° to 2100° R.

839

Pressures were measured throughout the engine on water, alkazine, and mercury manometers and were photographically recorded. Temperatures were measured and recorded by self-balancing potentiometers. Engine and tunnel operating conditions were indicated by gages on the engine control panel and were photographically recorded.

SYMBOLS

The following symbols are used in this report:

A	area, square feet
a	speed of sound in air, feet per second
D	compressor tip diameter, feet
g	acceleration due to gravity, feet per second per second
ghp	horsepower loss in high-speed reduction gear
H	enthalpy, Btu per pound
ΔH_{ad}	adiabatic enthalpy change, Btu per pound
J	mechanical equivalent of heat, foot-pounds per Btu
K, K_1	constants
M_c	compressor Mach number
N	engine speed, rpm
n	number of compressor stages
P	total pressure, pounds per square foot absolute
p	static pressure, pounds per square foot absolute
R	gas constant, foot-pounds per pound $^{\circ}F$
shp	shaft horsepower measured at torquemeter
T	total temperature, $^{\circ}R$
T_i	indicated temperature, $^{\circ}R$

U compressor tip speed, feet per second

W_a air flow, pounds per second

W_f fuel flow, pounds per hour

W_g gas flow, pounds per second

α thermocouple impact-recovery factor, 0.85

γ ratio of specific heats

δ ratio of compressor-inlet absolute total pressure to static pressure of NACA standard atmosphere at sea level

δ_5 ratio of turbine-inlet absolute total pressure to static pressure of NACA standard atmosphere at sea level

θ ratio of compressor-inlet absolute total temperature to static temperature of NACA standard atmosphere at sea level

θ_5 corrected ratio of turbine-inlet absolute total temperature to static temperature of NACA standard atmosphere at sea level, $(\gamma_5 T_5)/(1.40 \times 519)$

Ψ average compressor pressure coefficient per stage

η_c adiabatic compressor efficiency, percent

η_t adiabatic turbine efficiency, percent

Subscripts:

2 compressor inlet

3 compressor outlet

5 turbine inlet

6 turbine outlet

8 tail-pipe-nozzle outlet

c compressor

t turbine

METHOD OF CALCULATION

The total temperatures at the compressor inlet, the compressor outlet, and the tail-pipe-nozzle outlet were calculated from the relation

$$T = \frac{T_1 \left(\frac{P}{p}\right)^{\frac{\gamma-1}{\gamma}}}{1 + \alpha\left[\left(\frac{P}{p}\right)^{\frac{\gamma-1}{\gamma}} - 1\right]}$$

As in reference 1, the total enthalpy at the turbine inlet was assumed to be equal to the sum of the enthalpy at the tail-pipe-nozzle outlet and the drop in enthalpy across the turbine. The enthalpy drop across the turbine is equivalent to the sum of the enthalpy rise across the compressor, the shaft horsepower measured at the torquemeter, and the power loss in the high-speed reduction gear.

$$H_5 = H_8 + (H_3 - H_2) + \frac{550(shp + ghp)}{W_g J}$$

The turbine-inlet total temperature was then obtained from thermodynamic charts relating enthalpy and fuel-air ratio to temperature.

Air flow through the compressor was calculated from measurements at the compressor inlet by use of the equation

$$W_{a,2} = p_2 A_2 \sqrt{\frac{2\gamma_2 g}{(\gamma_2 - 1) RT_2}\left(\frac{P_2}{p_2}\right)^{\frac{\gamma_2-1}{\gamma_2}}\left[\left(\frac{P_2}{p_2}\right)^{\frac{\gamma_2-1}{\gamma_2}} - 1\right]}$$

Turbine gas flow was assumed equal to the sum of the compressor-inlet air flow and the engine fuel flow

$$W_g = W_a + \frac{W_f}{3600}$$

The adiabatic compressor efficiency was obtained from

$$\eta_c = \frac{\left[\left(\frac{P_3}{P_2}\right)^{\frac{\gamma_c-1}{\gamma_c}} - 1\right]}{\left[\left(\frac{T_3}{T_2}\right) - 1\right]} \times 100$$

where γ_c was assumed equal to 1.40.

Compressor Mach number, based on the total temperature of the air at the compressor inlet, was computed from

$$M_c = \frac{U}{a_2} = \frac{\pi\ DN}{60\sqrt{\gamma_2 g\ RT_2}}$$

The average compressor pressure coefficient per stage, which is defined as the ratio of the adiabatic work per stage to the work that would be required to accelerate the air to a velocity equal to the tip speed of the compressor, was obtained from

$$\Psi = \frac{\Delta H_{ad}}{n\frac{U^2}{2g}} = \frac{2}{n(\gamma_c - 1)}\ \frac{\left(\frac{P_3}{P_2}\right)^{\frac{\gamma_c-1}{\gamma_c}} - 1}{M_c^{\ 2}}$$

Adiabatic turbine efficiency was calculated from

$$\eta_t = \frac{T_5 - T_6}{T_5\left[1 - \left(\frac{P_6}{P_5}\right)^{\frac{\gamma_t-1}{\gamma_t}}\right]} \times 100$$

where γ_t was assumed equal to the average ratio of specific heats entering and leaving the turbine. Because the temperature drop through the tail pipe was small and the temperature measurements were more reliable at the tail-pipe-nozzle outlet than at the turbine outlet, T_6 was replaced by T_8 in the turbine-efficiency equation.

RESULTS AND DISCUSSION

Compressor and turbine performance characteristics for the range of conditions at which the axial-flow gas turbine-propeller engine was operated are discussed. Inasmuch as engine performance was obtained for a relatively small range of compressor-inlet ram-pressure ratios, no effort has been made to determine the effect of this parameter on the performance of the compressor and the turbine.

Compressor

The relation between corrected air flow, compressor Mach number, and corrected engine speed is shown in figure 11 for altitudes from 5000 to 35,000 feet. The air flows obtained at different altitudes generalized reasonably well and appear to be a function only of compressor Mach number for the range of operating conditions investigated.

During the operation of a compressor in a gas turbine-propeller engine, the compressor pressure ratio varies with the power delivered to the propeller. In order to increase the power delivered to the propeller at a particular engine speed, an increase in turbine-inlet temperature is necessary, which in turn increases the turbine-inlet pressure. This rise in turbine-inlet pressure results in an increase in compressor-outlet pressure and, consequently, compressor pressure ratio.

It can be analytically shown that, for conditions at which the turbine nozzles are choked and the corrected air flow is constant, the compressor pressure ratio is proportional to the square root of the corrected turbine-inlet temperature. When the pressure ratio across the turbine nozzle exceeds the critical value (about 1.89), the mass flow through the turbine nozzles can be expressed as

$$W_g = \frac{K\ A_5\ P_5 \sqrt{\gamma_5}}{\sqrt{T_5}}$$

If the air flow through the engine is assumed equal to the gas flow and the correction factors δ and θ are applied to this equation, the corrected air flow becomes

$$\frac{W_a \sqrt{\theta}}{\delta} = K_1 A_5 \frac{P_5 \sqrt{\gamma_5}}{P_2 \sqrt{T_5/T_2}}$$

As a first-order approximation, the compressor-outlet total pressure P_3 may be assumed equal to the turbine-inlet total pressure P_5. The variation in $\sqrt{\gamma_5}$ was also assumed to be negligible. Consequently, at a constant corrected air flow,

$$\frac{P_3}{P_2} \propto \sqrt{\frac{T_5}{T_2}}$$

and because $\theta = \frac{T_2}{519}$

$$\frac{P_3}{P_2} \propto \sqrt{\frac{T_5}{\theta}}$$

The compressor pressure ratio is plotted in figure 12 against the square root of the corrected turbine-inlet temperature for constant corrected air flows from 8.8 to 23.7 pounds per second, which were obtained at altitudes from 5000 to 35,000 feet. The compressor pressure ratio is shown to increase linearly with the square root of the corrected turbine-inlet temperature at a constant corrected air flow. For the range of conditions investigated, a maximum compressor pressure ratio of 6.15 was obtained with a corrected air flow of 23.7 pounds per second at a corrected turbine-inlet temperature of 2475° R.

The compressor efficiency was determined by plotting the actual temperature-rise factor $(T_3/T_2) - 1$ against the adiabatic temperature-rise factor $(P_3/P_2)^{\frac{\gamma_c - 1}{\gamma_c}} - 1$, as shown in figure 13. A single curve was faired through all the data points, inasmuch as the data scatter did not allow separation of the effects of turbine-inlet temperature and altitude on compressor efficiency at a particular value of compressor pressure ratio. A cross plot of the data from figures 12 and 13 in figure 14 shows the variation of compressor efficiency with corrected air flow for constant values of corrected turbine-inlet temperatures from 1600° to 2400° R. For the range of air flows investigated, the compressor efficiency was not greatly affected by changes in turbine-inlet temperature. A maximum compressor efficiency of about 77 percent

occurred at a corrected air flow of approximately 20 pounds per second for corrected turbine-inlet temperatures from 1800° to 2200° R. This peak efficiency may be somewhat low because of dirt and oil deposits on the stator and rotor blades.

The compressor-performance-characteristic curves for the range of engine operating conditions investigated were obtained by cross-plotting the data from figures 11, 12, and 14 in figure 15. The compressor pressure ratio increased with an increase in corrected air flow at constant values of corrected turbine-inlet temperature. The maximum compressor efficiencies occurred near the value of corrected air flow corresponding to a corrected engine speed of 13,000 rpm.

The variation of compressor pressure coefficient with corrected turbine-inlet temperature is shown in figure 16 for constant values of corrected air flow. The compressor pressure coefficient increased with the corrected turbine-inlet temperature. A cross plot (fig. 17) of the data from figure 16 shows the variation of compressor pressure coefficient with corrected air flow for constant values of corrected turbine-inlet temperature. A maximum pressure coefficient of 0.322 was obtained at a corrected air flow of about 14 pounds per second and a corrected turbine-inlet temperature of 2000° R. The maximum pressure coefficient does not occur at rated engine operating conditions.

Turbine

Turbine pressure ratio and corrected turbine speed are plotted as functions of corrected turbine-inlet temperature in figure 18 for constant values of corrected engine speed at altitudes from 5000 to 35,000 feet. The highest turbine pressure ratio at which data were obtained was 4.65 at a corrected turbine speed of 6700 rpm and a corrected turbine-inlet temperature of 2475° R. A cross plot of these data (fig. 19) shows the variation of turbine pressure ratio with corrected turbine speed for corrected turbine-inlet temperatures from 1600° to 2400° R. The turbine pressure ratio increased with an increase in corrected turbine speed and corrected turbine-inlet temperature. At a corrected turbine speed of 6800 rpm, an increase in corrected turbine-inlet temperature from 1600° to 2400° R raised the turbine pressure ratio from 3.05 to 4.50.

The turbine efficiencies were obtained by a method similar to that used in determining the compressor efficiencies. The actual

temperature-drop factor $1 - (T_8/T_5)$ is plotted against the adiabatic temperature-drop factor $1 - (P_6/P_5)^{\frac{\gamma_t - 1}{\gamma_t}}$ in figure 20 for altitudes from 5000 to 35,000 feet. Lines of constant turbine efficiency superimposed on the data show that practically all the turbine efficiencies were between 76 and 82 percent. It is also shown that the turbine efficiencies were not noticeably affected by changes in altitude.

In order to show turbine efficiency as a function of corrected turbine speed and to determine the effect of turbine-inlet temperature on turbine efficiency, the actual and adiabatic temperature-drop factors first had to be plotted against the corrected turbine-inlet temperature for constant values of corrected engine speed, as shown in figure 21. A cross plot of the data from figures 18 and 21 in figure 22 shows the turbine efficiency as a function of corrected turbine speed. Although the data from figures 18 and 21 varied by about 1.5 percent from the curve shown in figure 22, no consistent variation of turbine efficiency with turbine-inlet temperature was apparent for the range of conditions investigated. The faired curve in figure 22 indicates a maximum turbine efficiency of 81.5 percent at corrected turbine speeds from 6200 to 7400 rpm. This range of corrected turbine speeds includes engine operation at rated speed for all altitudes and turbine-inlet temperatures investigated.

The variation of turbine pressure ratio with corrected gas flow is shown in figure 23 for altitudes from 5000 to 35,000 feet. For practically all the conditions investigated, the corrected gas flow was constant, which indicates that the turbine nozzles were choked. A corrected gas flow of about 9 pounds per second was obtained for turbine pressure ratios from approximately 2.0 to 4.65.

SUMMARY OF RESULTS

Compressor and turbine performance characteristics were obtained as part of an investigation of an axial-flow gas turbine-propeller engine in the Cleveland altitude wind tunnel. Data were obtained at altitudes from 5000 to 35,000 feet, engine speeds from 8000 to 13,000 rpm, turbine-inlet temperatures from 1400° to 2100° R, and a compressor-inlet ram-pressure ratio of 1.00. The following results were obtained:

839

1. For the range of operating conditions investigated, a maximum compressor pressure ratio of 6.15 was obtained at a corrected air flow of 23.7 pounds per second and a corrected turbine-inlet temperature of 2475° R.

2. Peak adiabatic compressor efficiencies of about 77 percent were obtained near the value of corrected air flow corresponding to a corrected engine speed of 13,000 rpm. This value of maximum efficiency may be somewhat low, however, because of dirt accumulation on the compressor blades.

3. A maximum compressor pressure coefficient of 0.322 was obtained at a corrected air flow of about 14 pounds per second and a corrected turbine-inlet temperature of 2000° R. The peak compressor pressure coefficient did not occur at rated engine operating conditions.

4. A maximum adiabatic turbine efficiency of 81.5 percent was obtained at rated engine speed for all altitudes and turbine-inlet temperatures investigated.

Flight Propulsion Research Laboratory,
National Advisory Committee for Aeronautics,
Cleveland, Ohio.

REFERENCES

1. Saari, Martin J., and Wallner, Lewis E.: Preliminary Results of an Altitude-Wind-Tunnel Investigation of an Axial-Flow Gas Turbine-Propeller Engine. I - Performance Characteristics. NACA RM No. E8F10, 1948.

2. Conrad, E. W., and Durham, J. D.: Preliminary Results of an Altitude-Wind-Tunnel Investigation of an Axial-Flow Gas Turbine-Propeller Engine. II - Windmilling Characteristics. NACA RM No. E8F10a, 1948.

3. Geisenheyner, Robert M., and Berdysz, Joseph J.: Preliminary Results of an Altitude-Wind-Tunnel Investigation of an Axial-Flow Gas Turbine-Propeller Engine. III - Pressure and Temperature Distribution. NACA RM No. E8F10b, 1948.

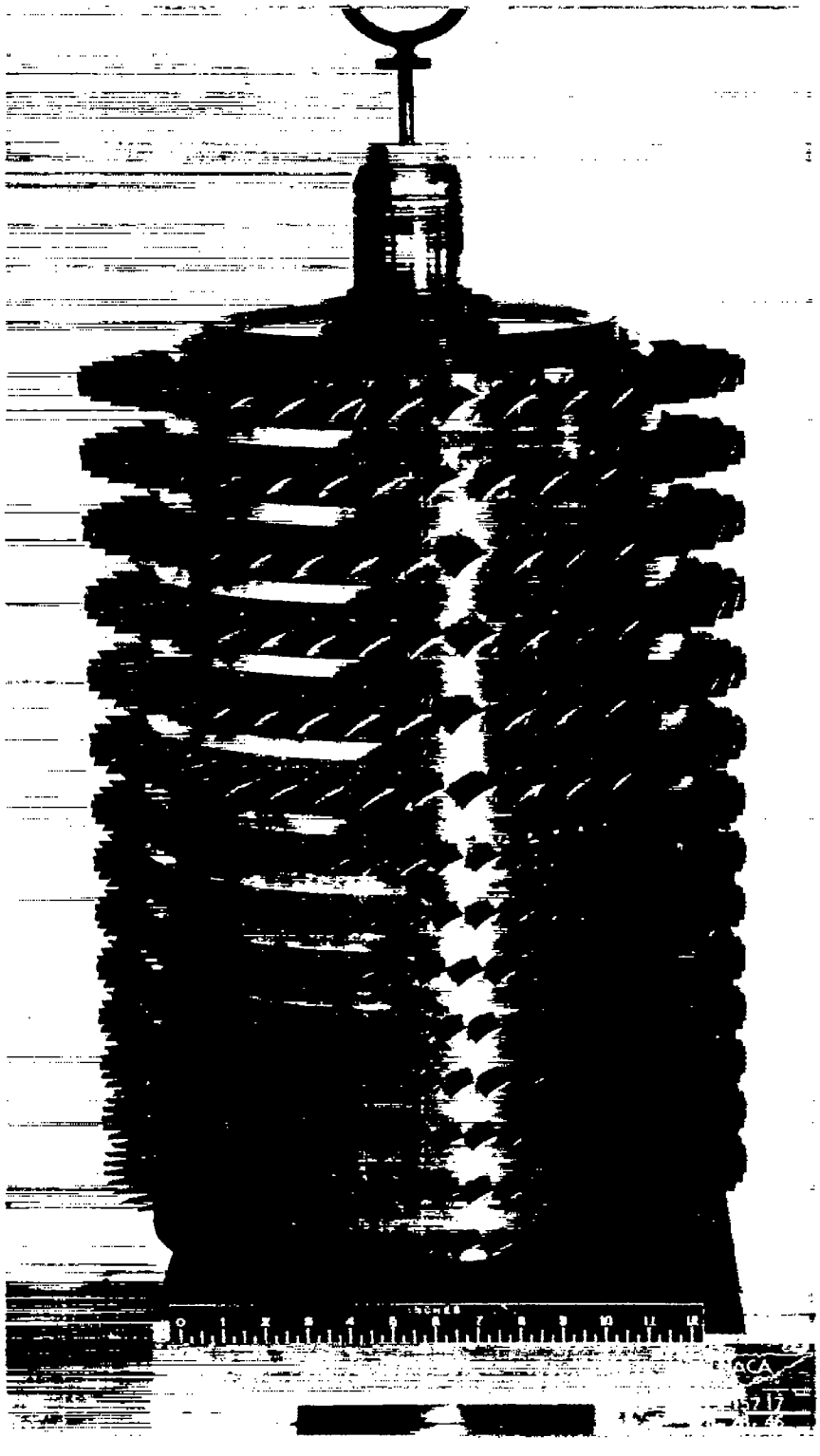

Figure 1. - Compressor rotor of axial-flow gas turbine-propeller engine.

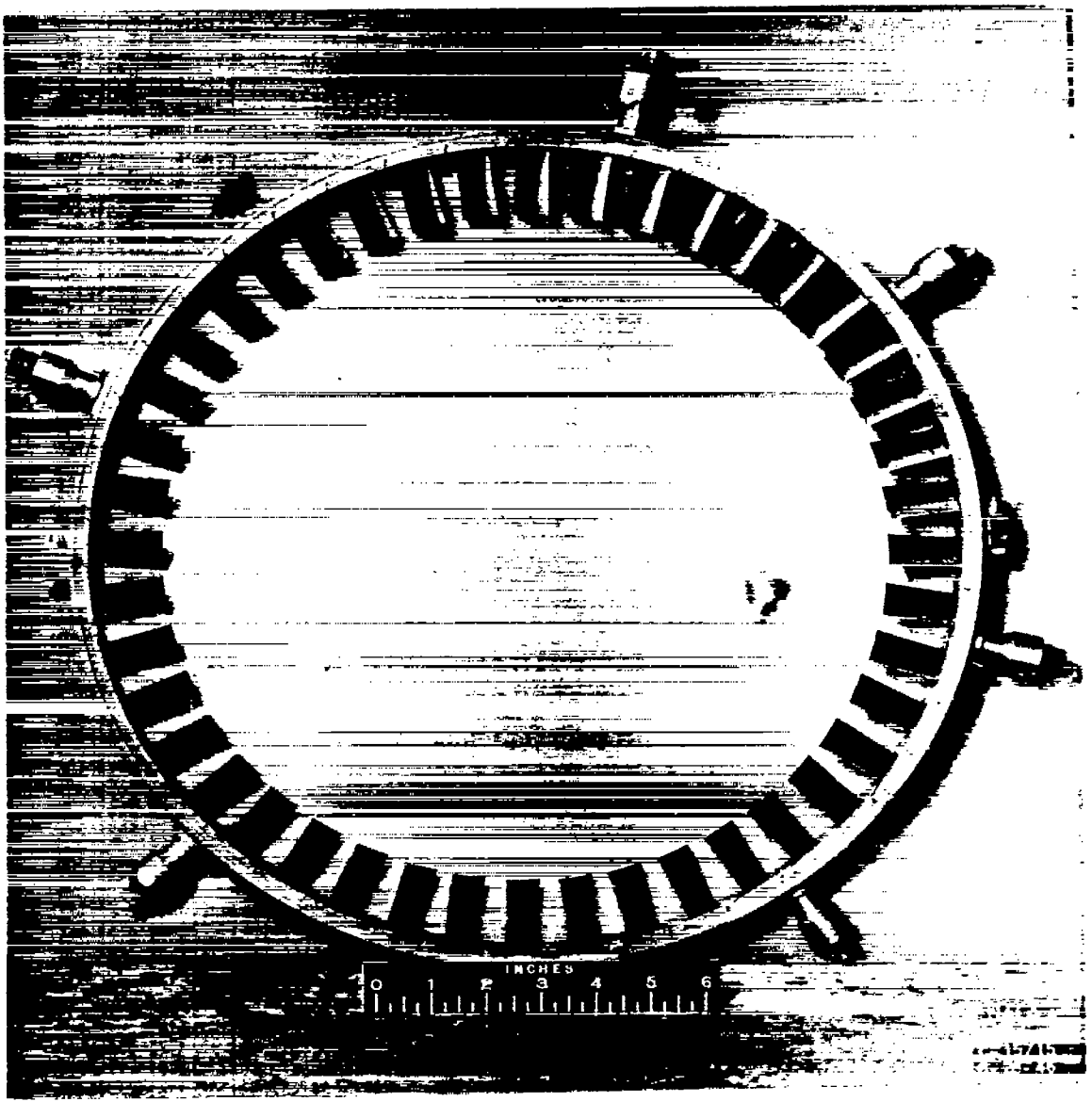

Figure 2. - Sixth-stage stator ring from compressor of axial-flow gas turbine-propeller engine.

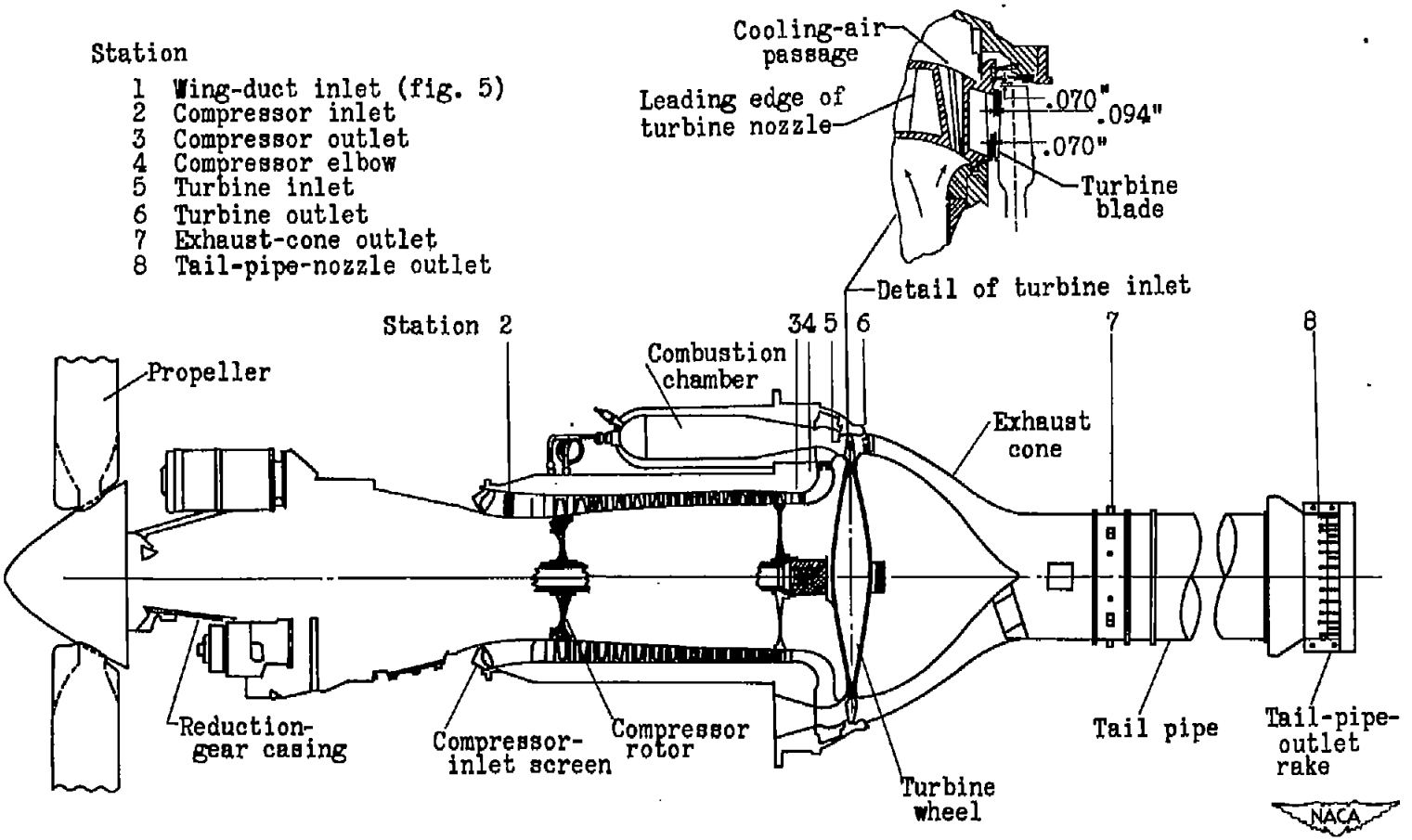

Figure 3. - Side view of axial-flow gas turbine-propeller engine showing location of measuring stations.

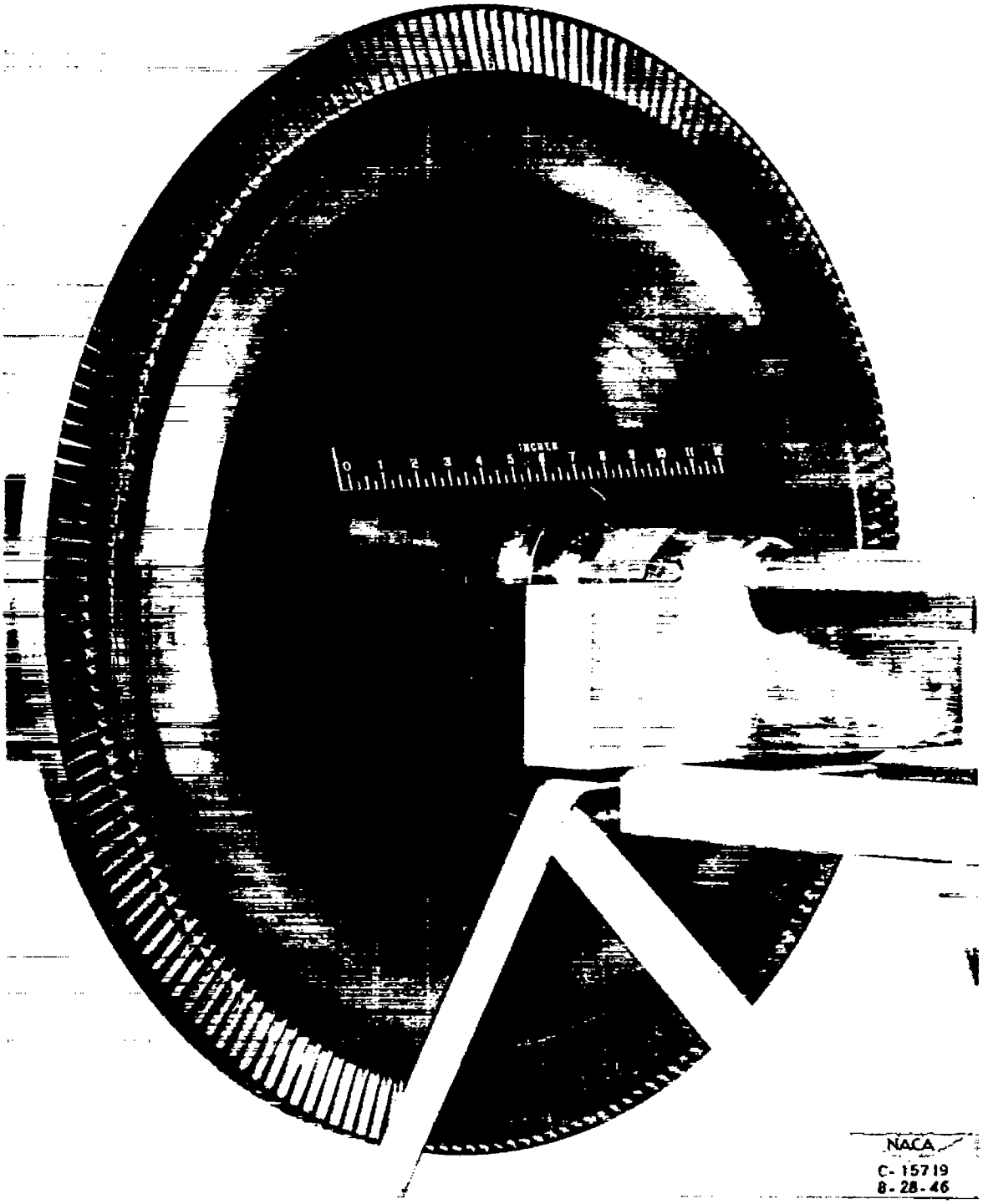

Figure 4. - Turbine wheel used in axial-flow gas turbine-propeller engine.

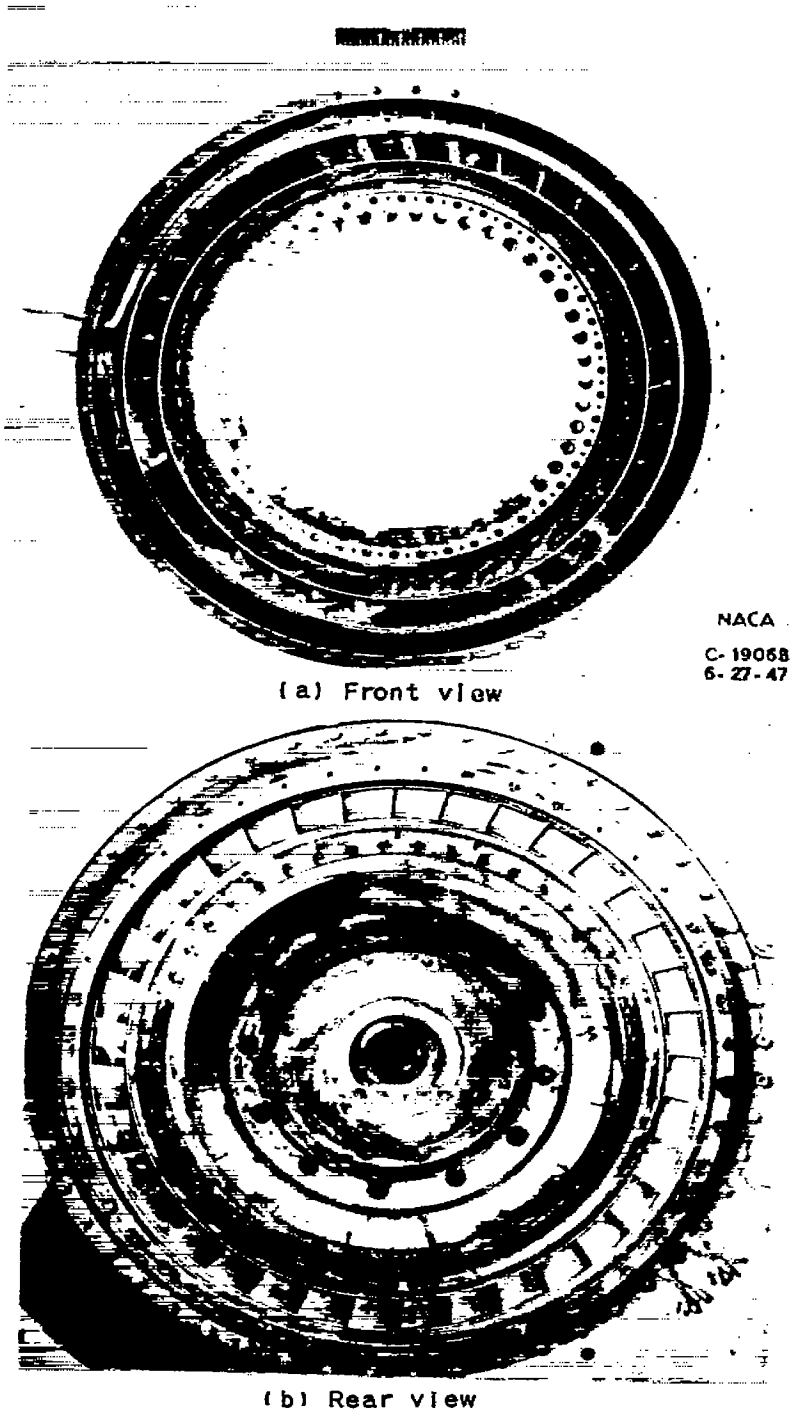

(a) Front view

(b) Rear view

Figure 5. - Turbine nozzle of axial-flow gas turbine-propeller engine.

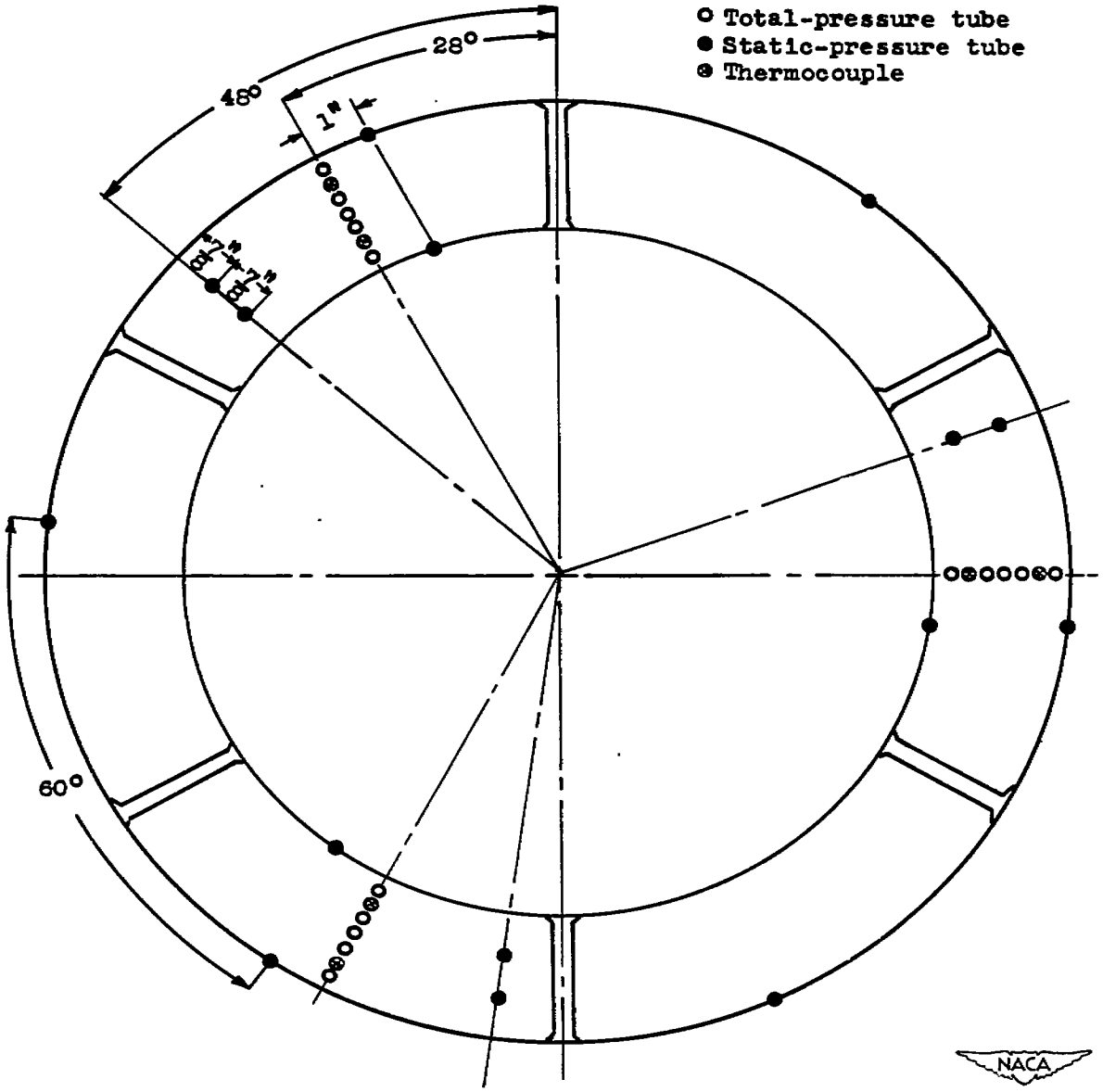

Figure 6. – Location of instrumentation at compressor inlet, looking aft, station 2.

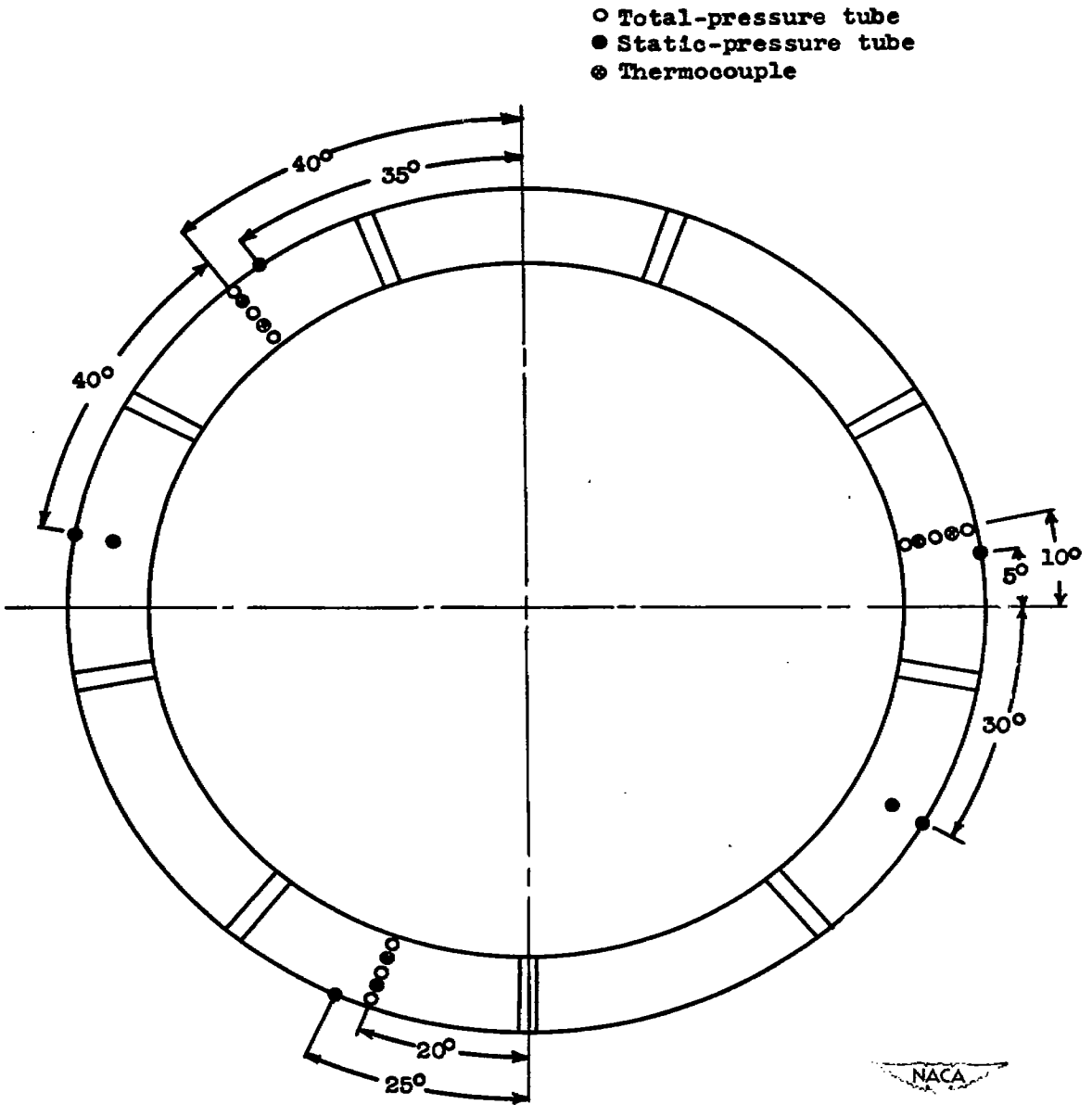

Figure 7. - Location of instrumentation at compressor outlet, looking aft, station 3.

839

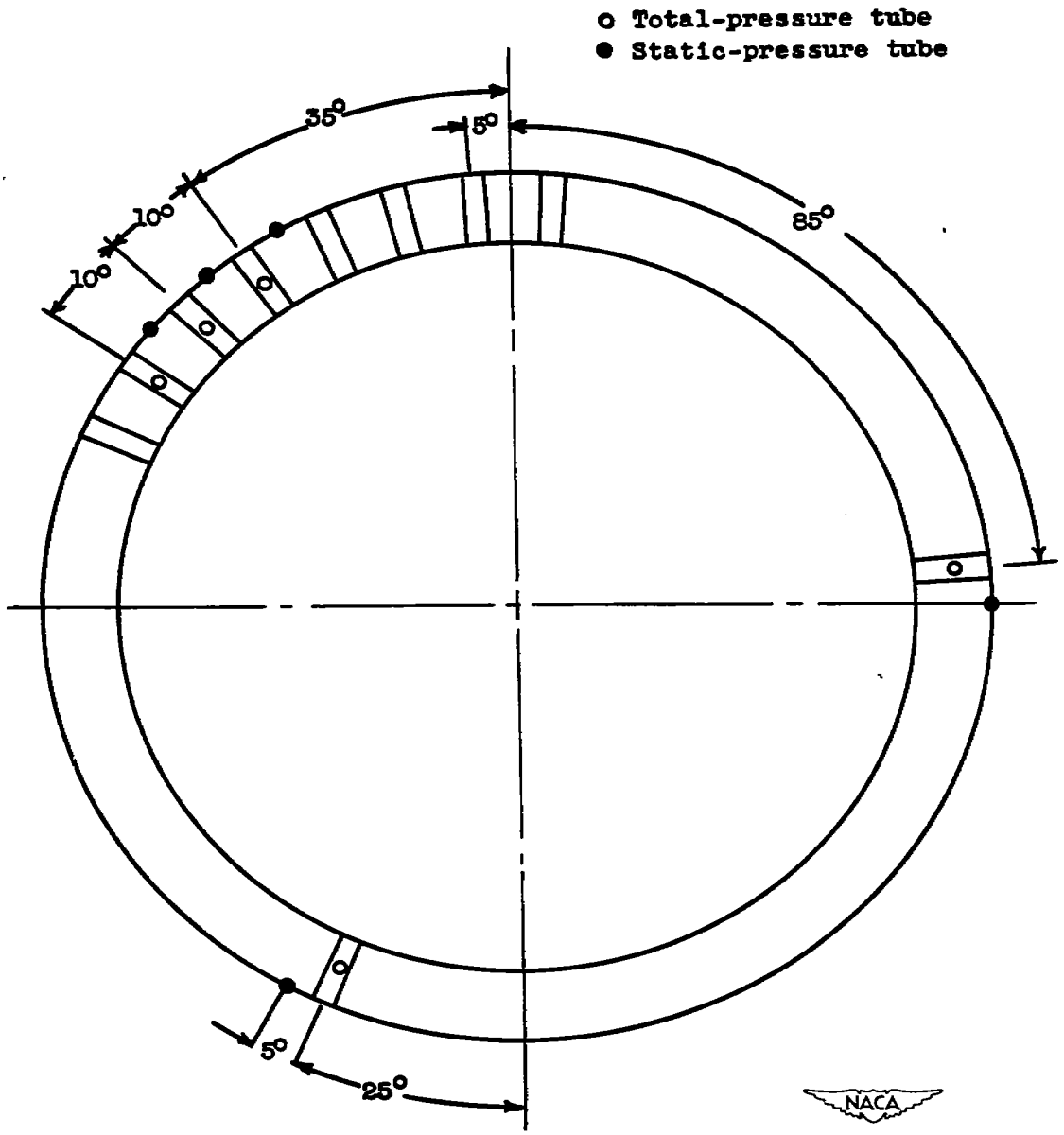

Figure 8. - Location of instrumentation at turbine inlet, looking aft, station 5.

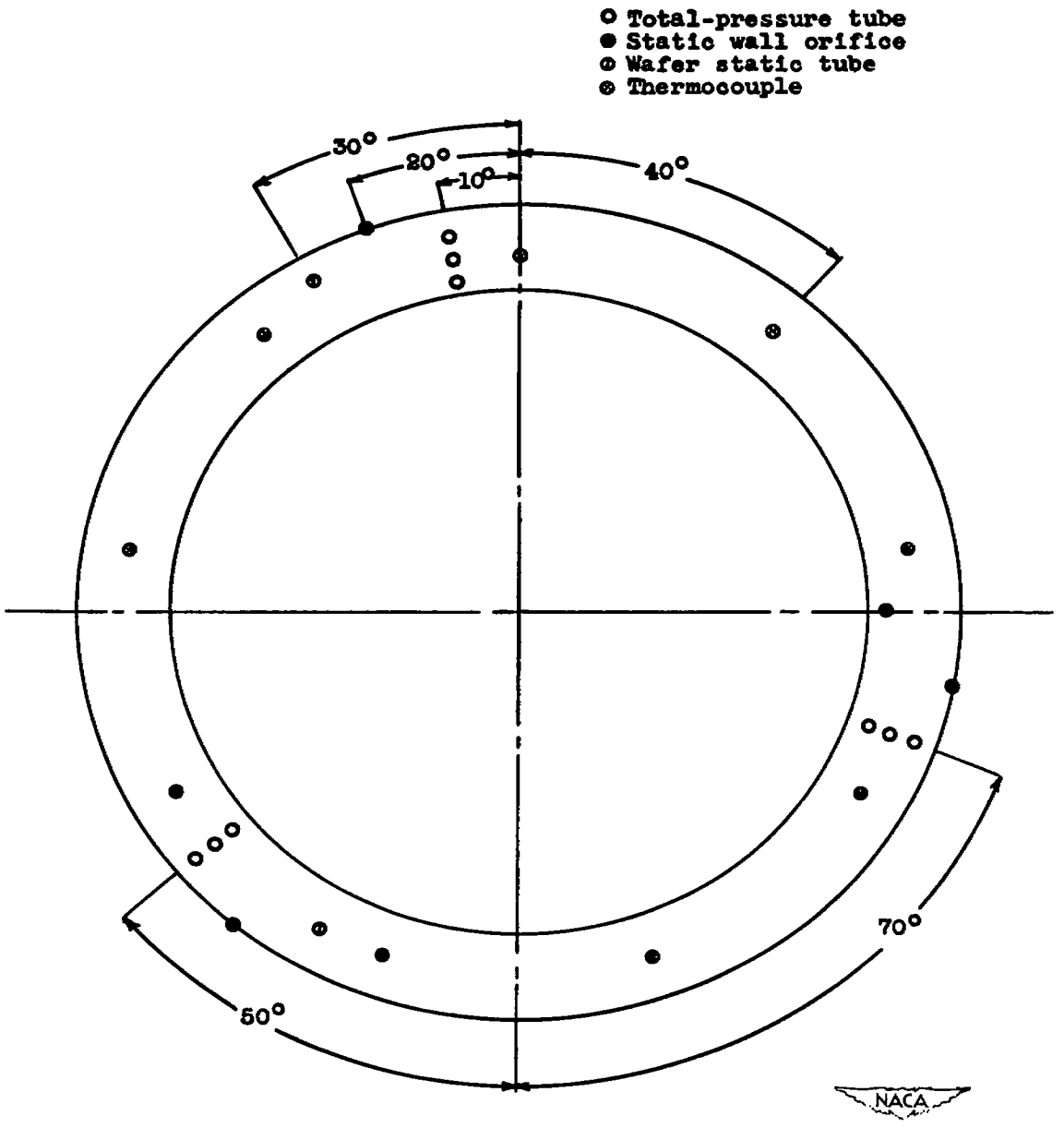

Figure 9. - Location of instrumentation at turbine outlet, looking aft, station 6.

839

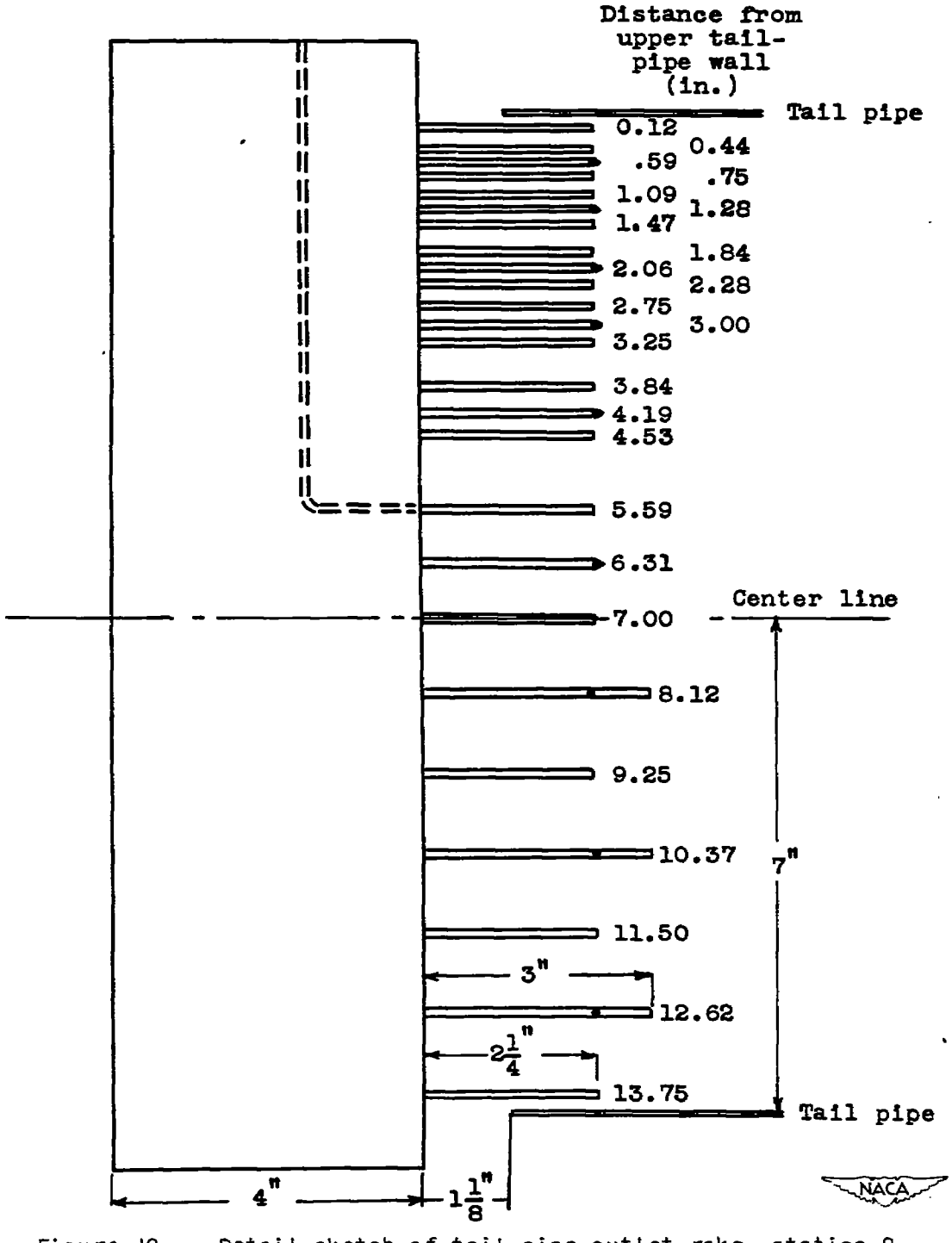

Figure 10. - Detail sketch of tail-pipe-outlet rake, station 8.

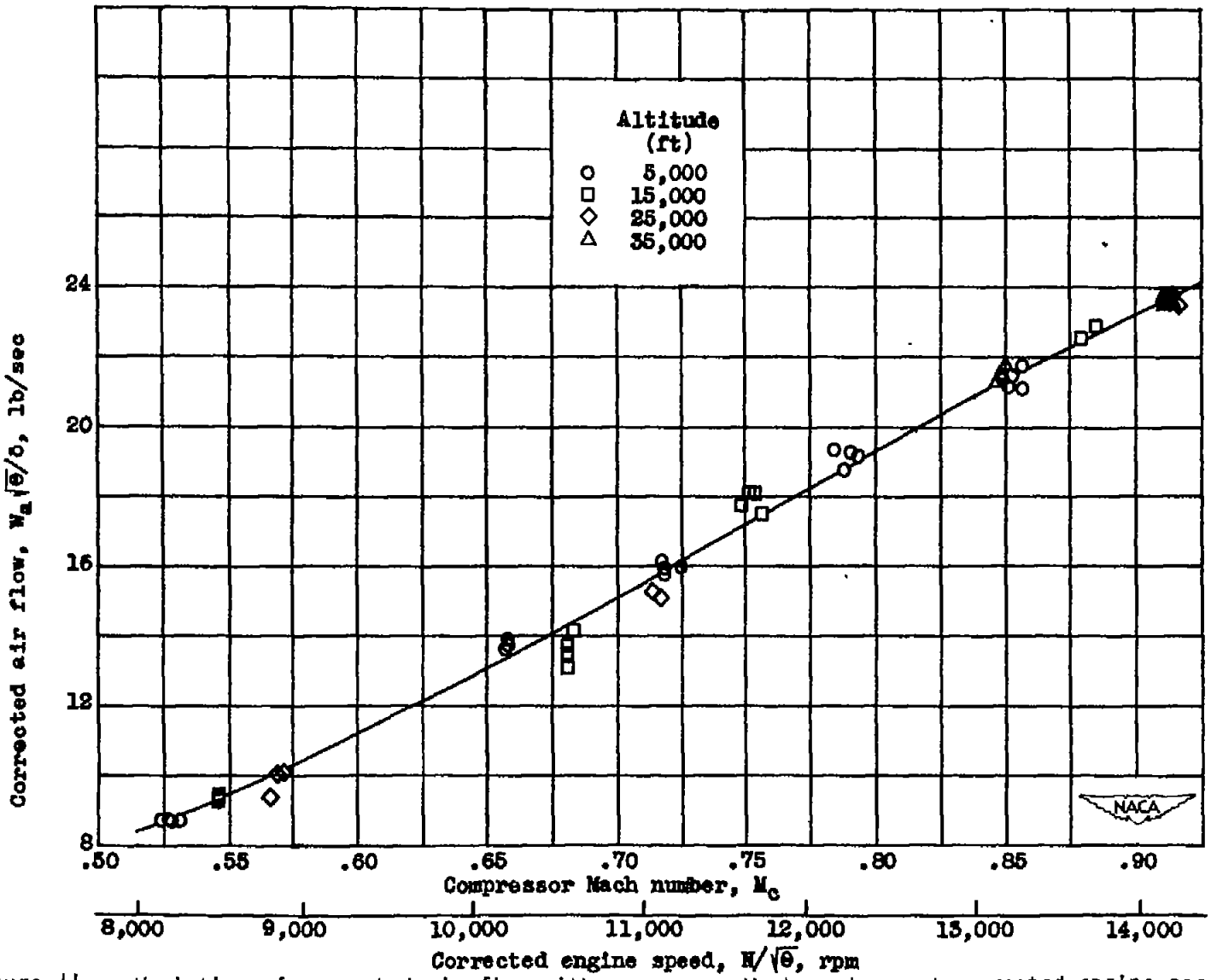

Figure 11. - Variation of corrected air flow with compressor Mach number and corrected engine speed. Compressor-inlet ram-pressure ratio, 1.00.

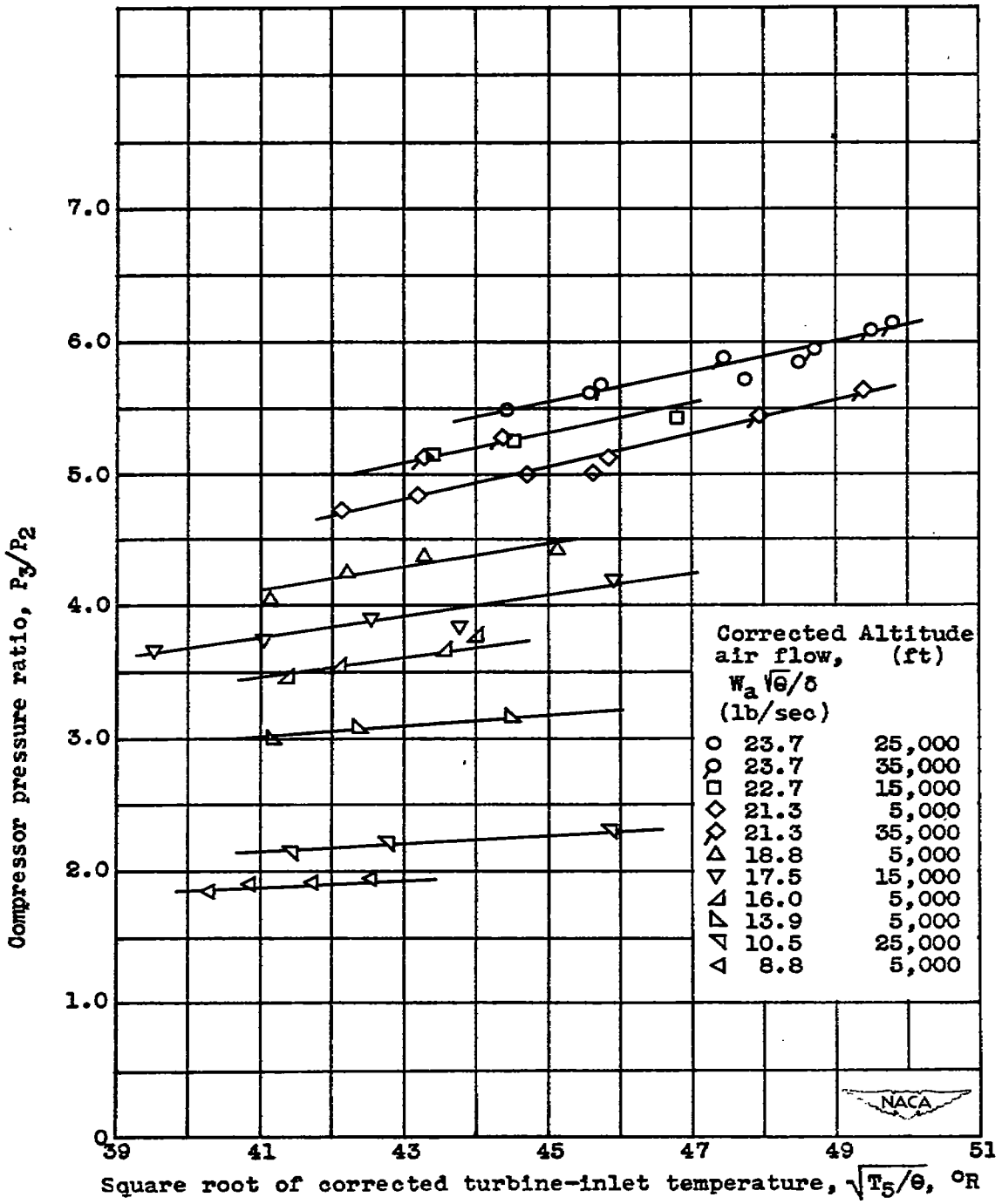

Figure 12. - Variation of compressor pressure ratio with square root of corrected turbine-inlet temperature. Compressor-inlet ram-pressure ratio, 1.00.

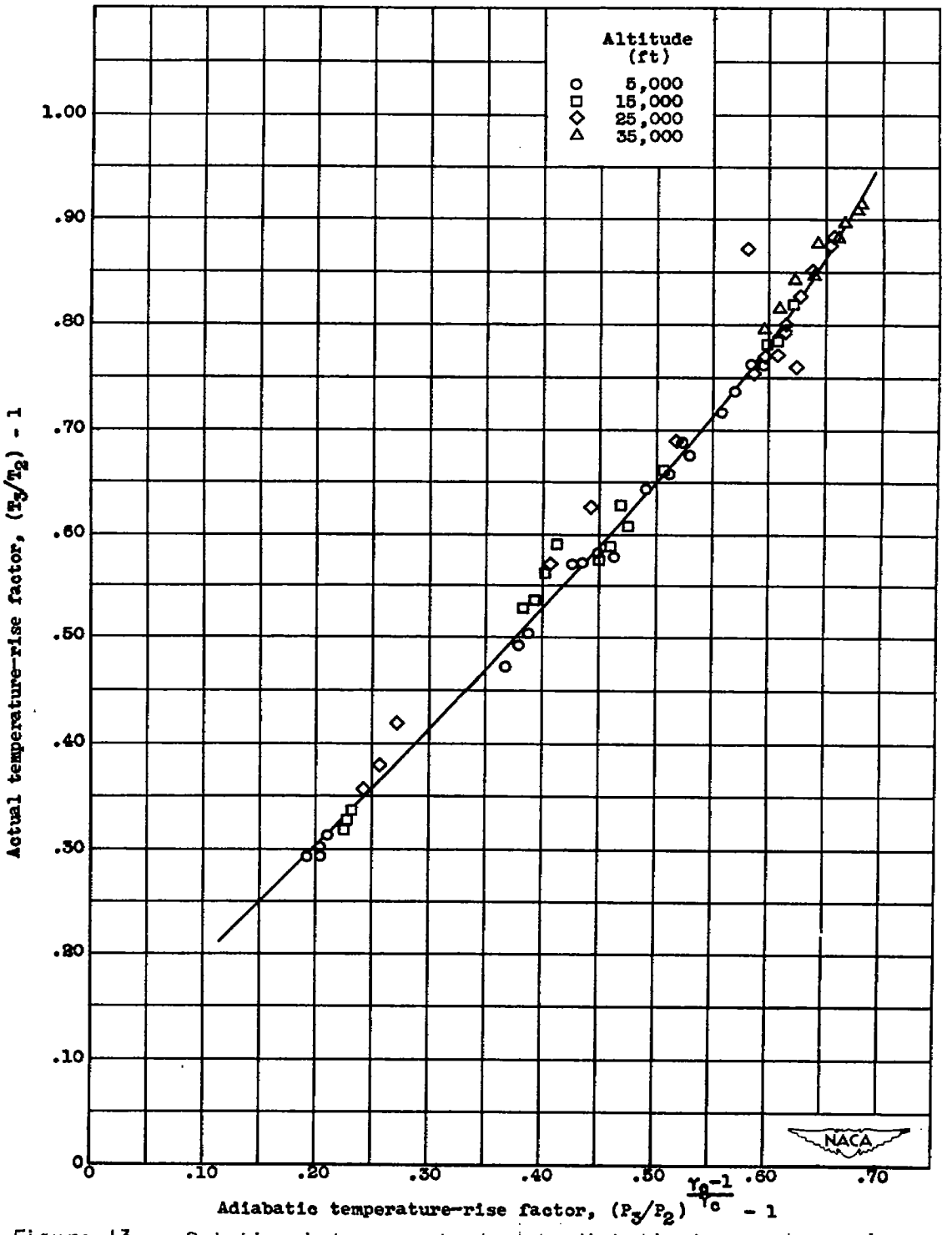

Figure 13. - Relation between actual and adiabatic temperature-rise factors. Compressor-inlet ram-pressure ratio, 1.00.

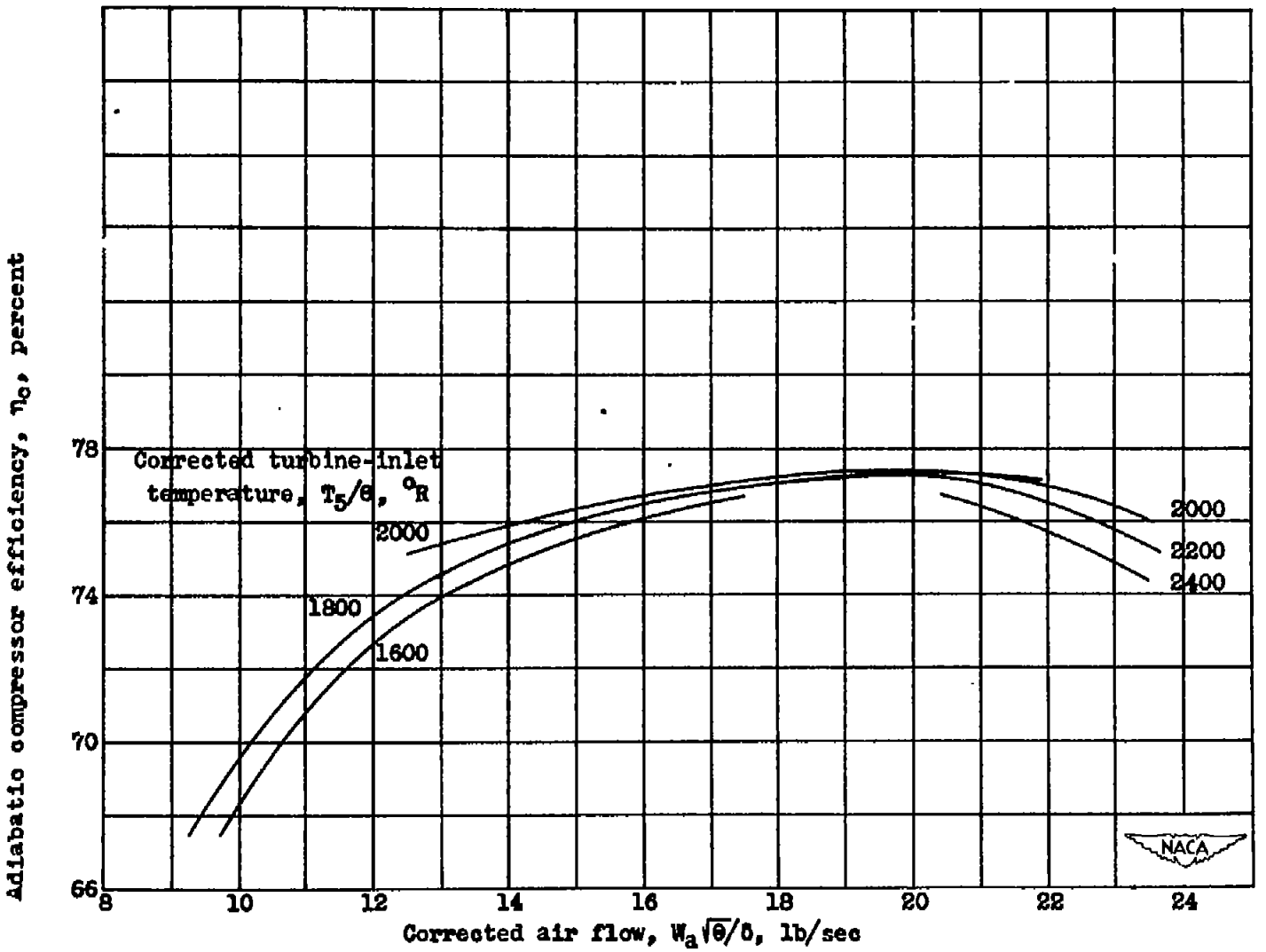

Figure 14. - Variation of adiabatic compressor efficiency with corrected air flow. Compressor-inlet ram-pressure ratio, 1.00.

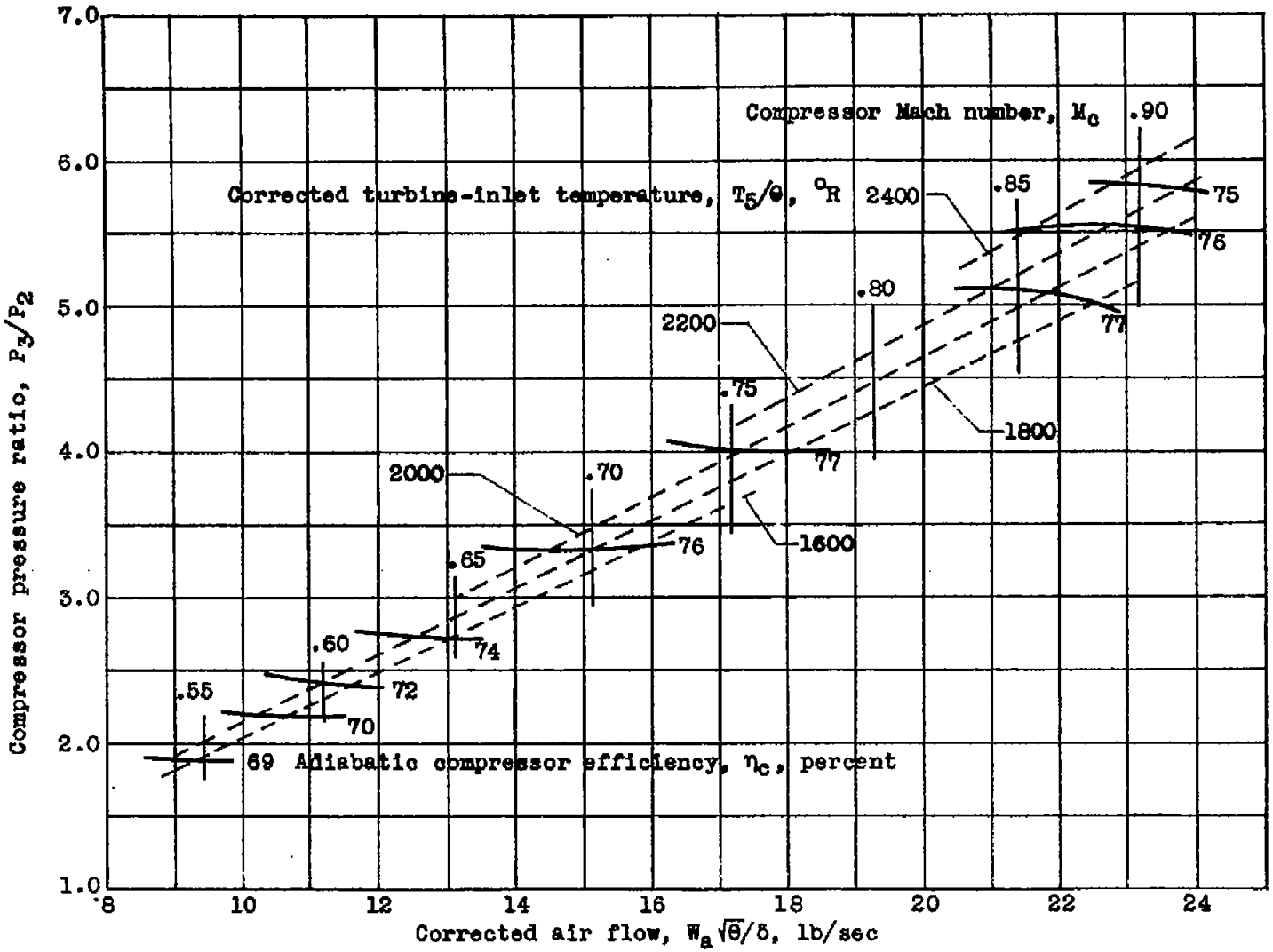

Figure 15. - Compressor-performance-characteristic curves for operating range of axial-flow gas turbine-propeller engine. Compressor-inlet ram-pressure ratio, 1.00.

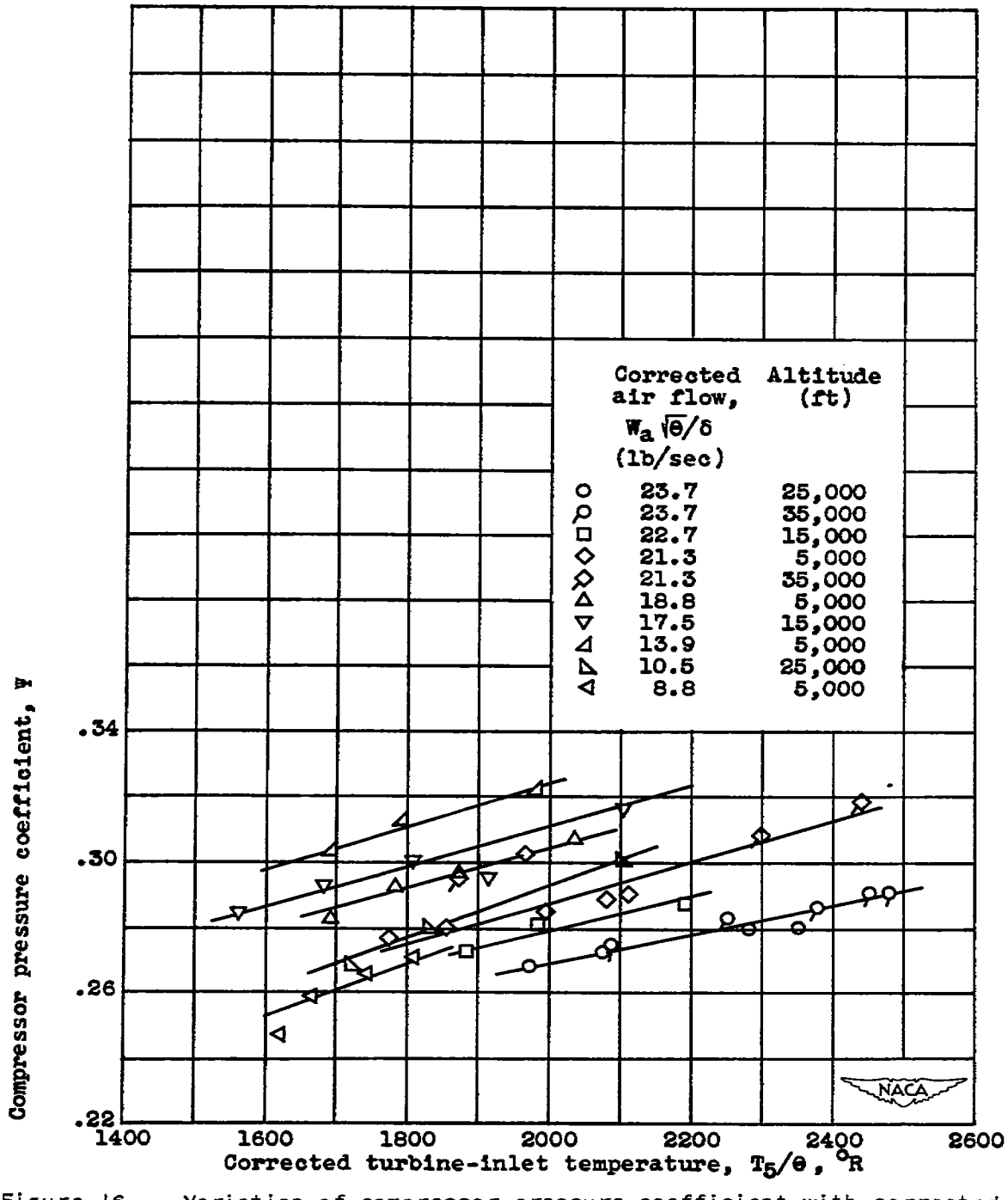

Figure 16. - Variation of compressor pressure coefficient with corrected turbine-inlet temperature. Compressor-inlet Mach number, 1.00.

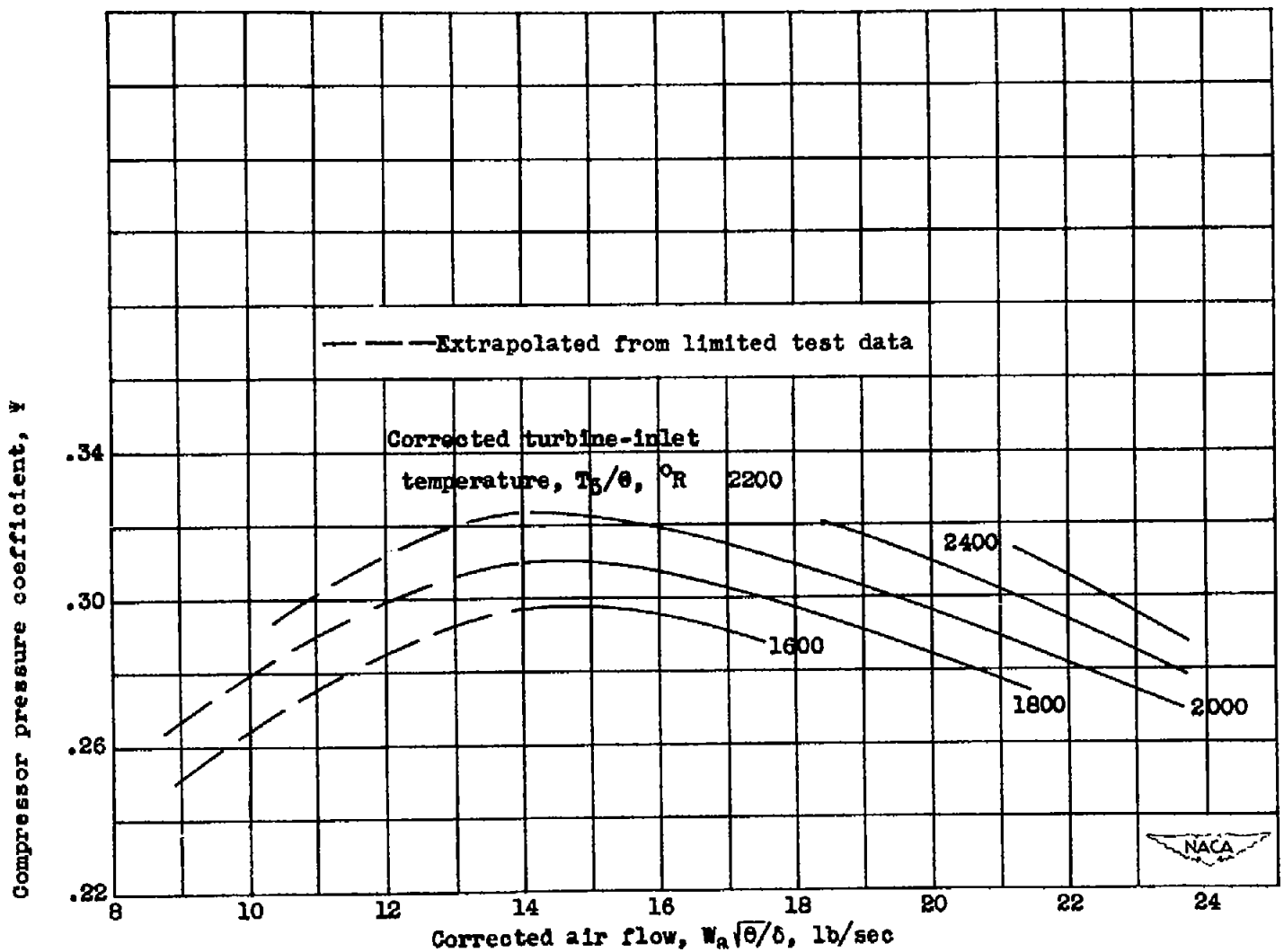

Figure 17. - Variation of compressor pressure coefficient with corrected air flow. Compressor-inlet ram-pressure ratio, 1.00.

839

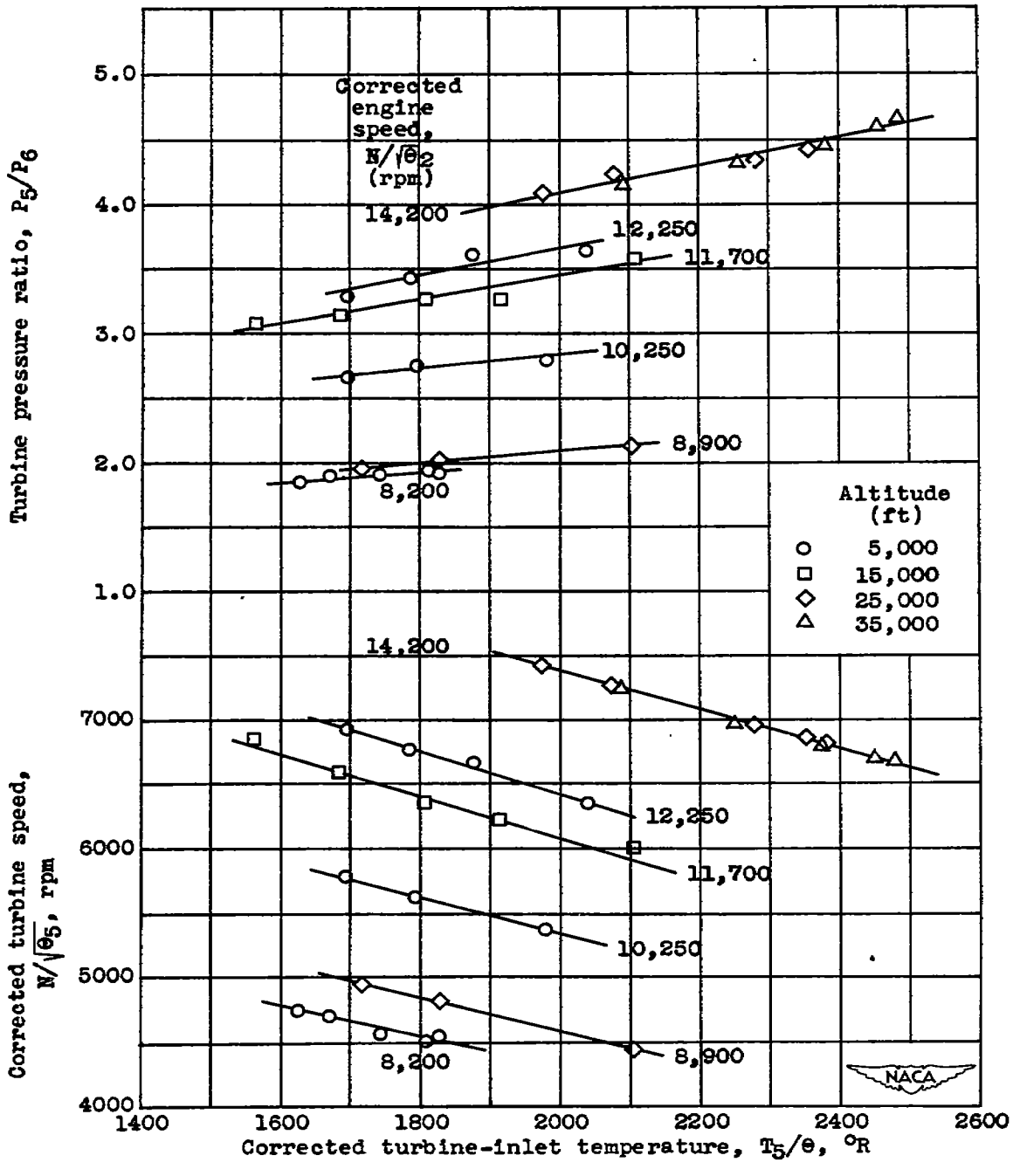

Figure 18. - Variation of corrected turbine speed and turbine pressure ratio with corrected turbine-inlet temperature. Compressor-inlet ram-pressure ratio, 1.00.

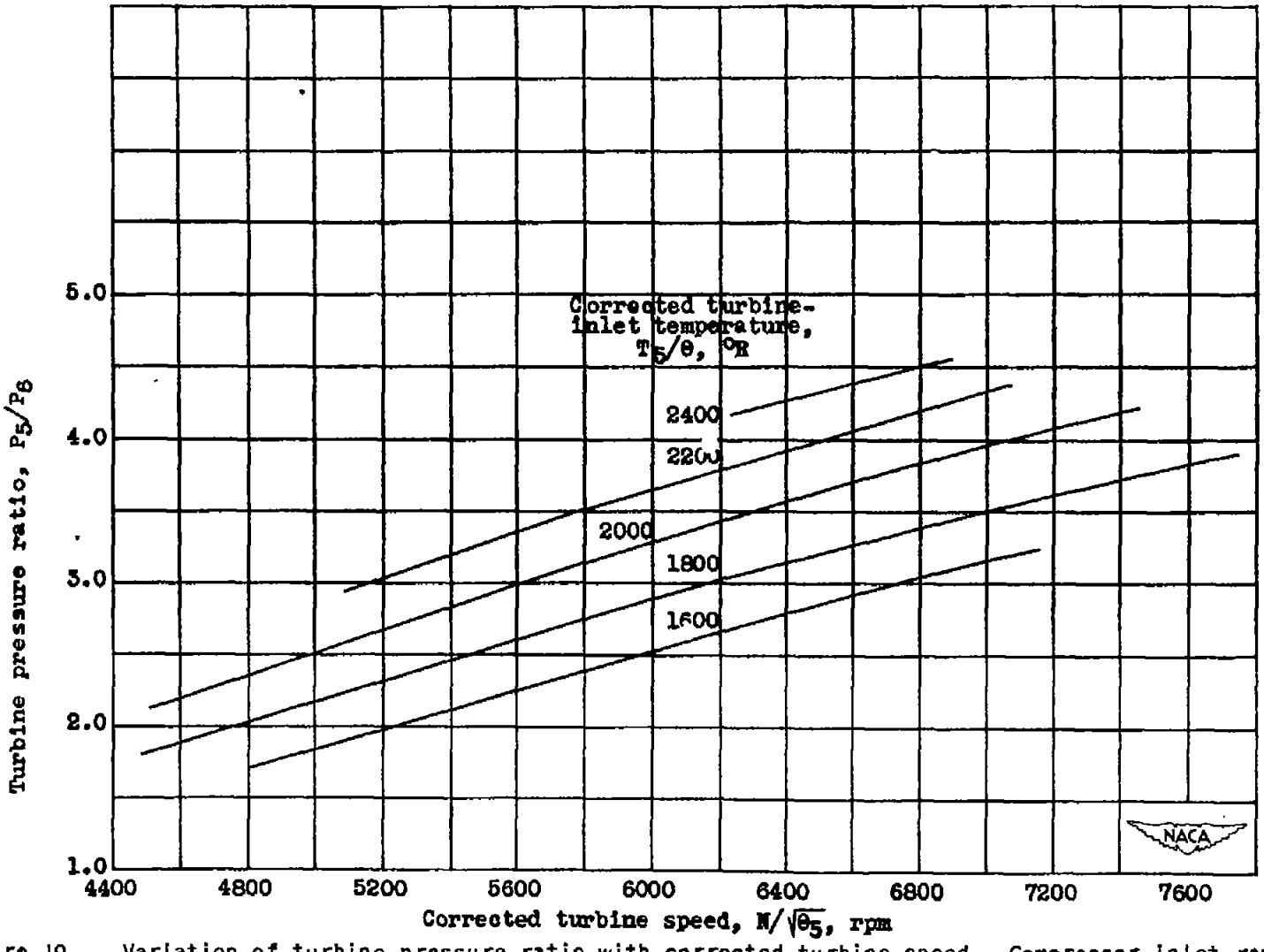

Figure 19. - Variation of turbine pressure ratio with corrected turbine speed. Compressor-inlet ram-pressure ratio, 1.00

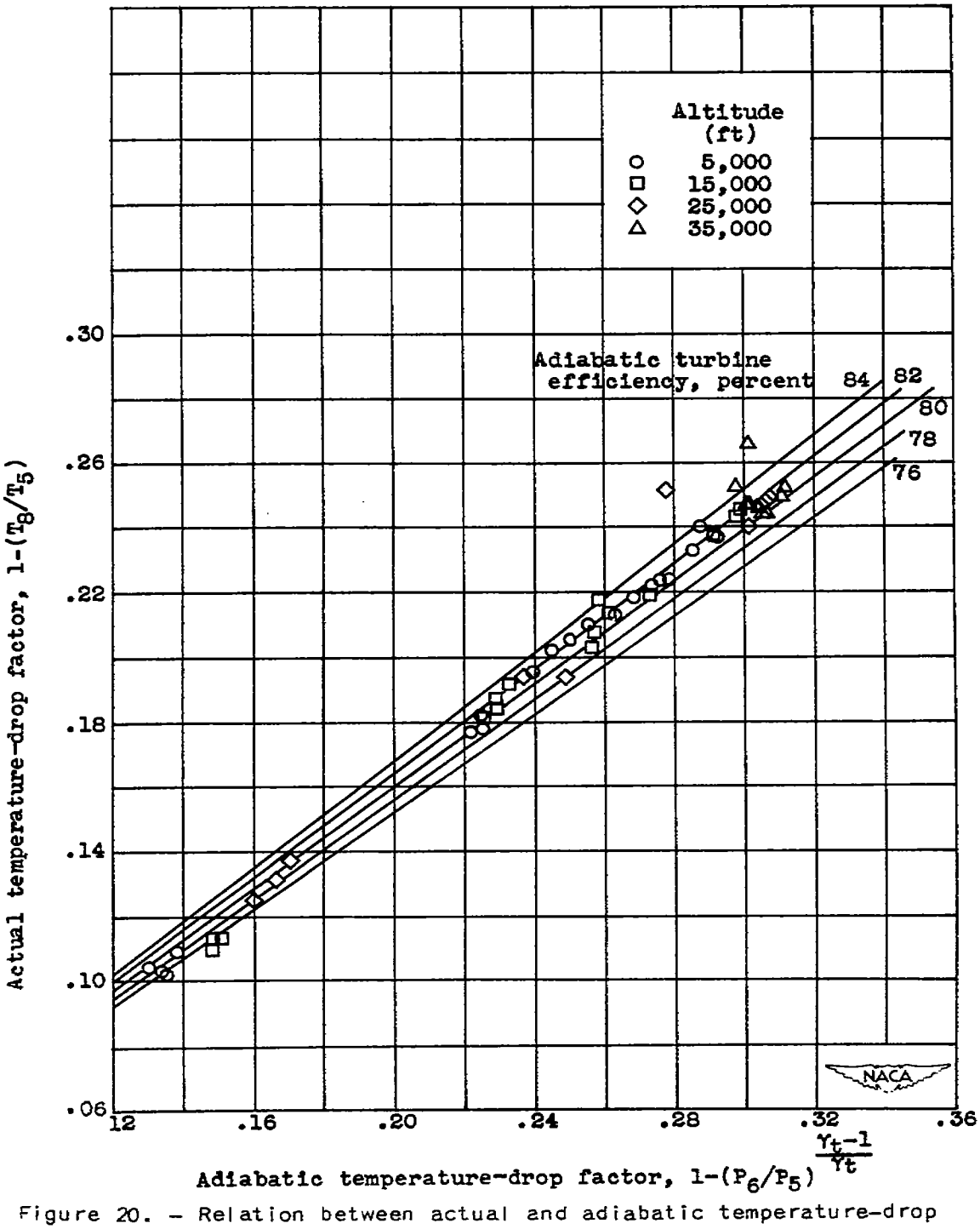

Figure 20. - Relation between actual and adiabatic temperature-drop factors. Compressor-inlet ram-pressure ratio, 1.00.

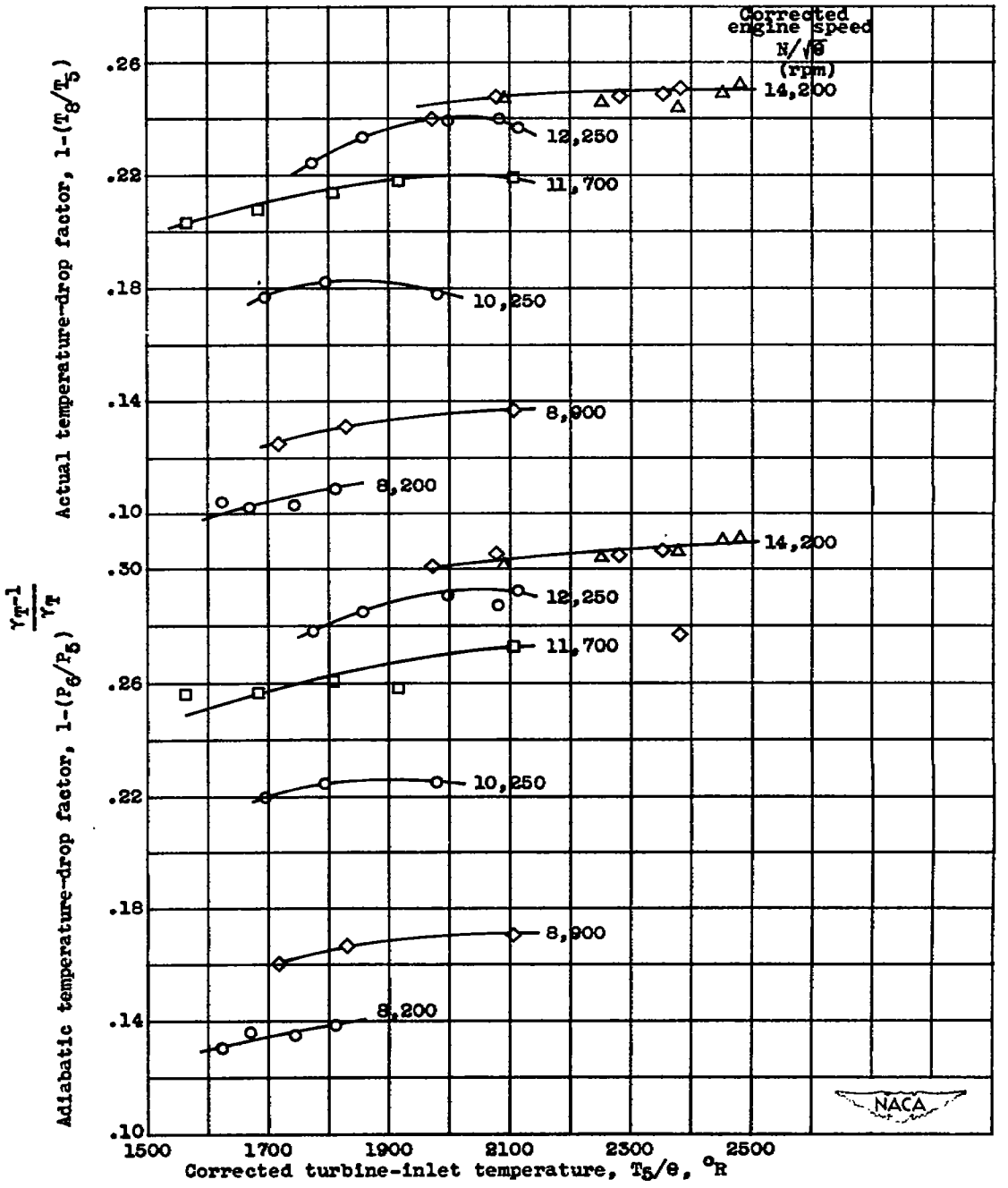

Figure 21. - Variation of actual and adiabatic temperature-drop factors with corrected turbine-inlet temperature. Compressor-inlet ram-pressure ratio, 1.00.

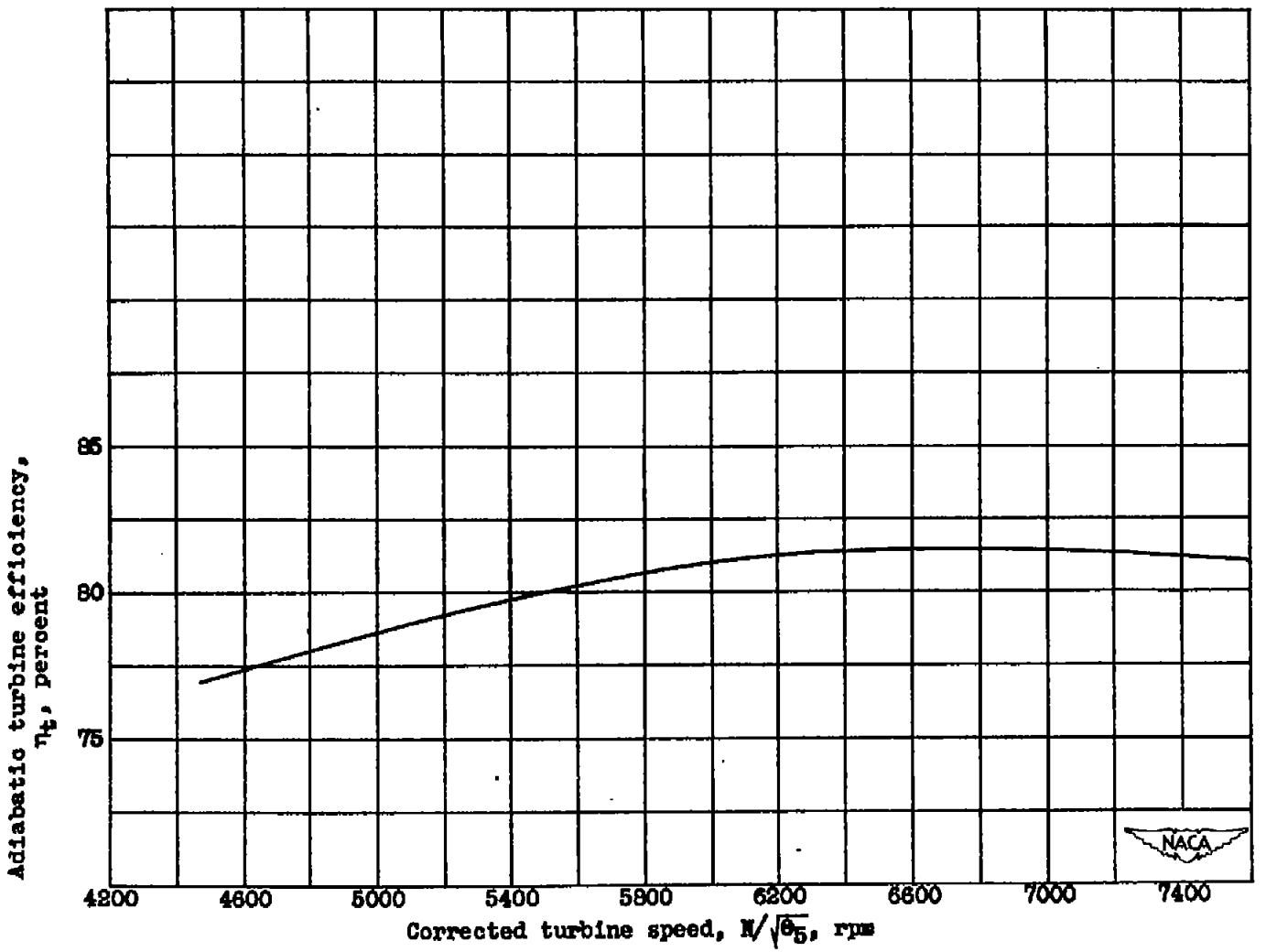

Figure 22. - Variation of adiabatic turbine efficiency with corrected turbine speed. Compressor-inlet ram-pressure ratio, 1.00.

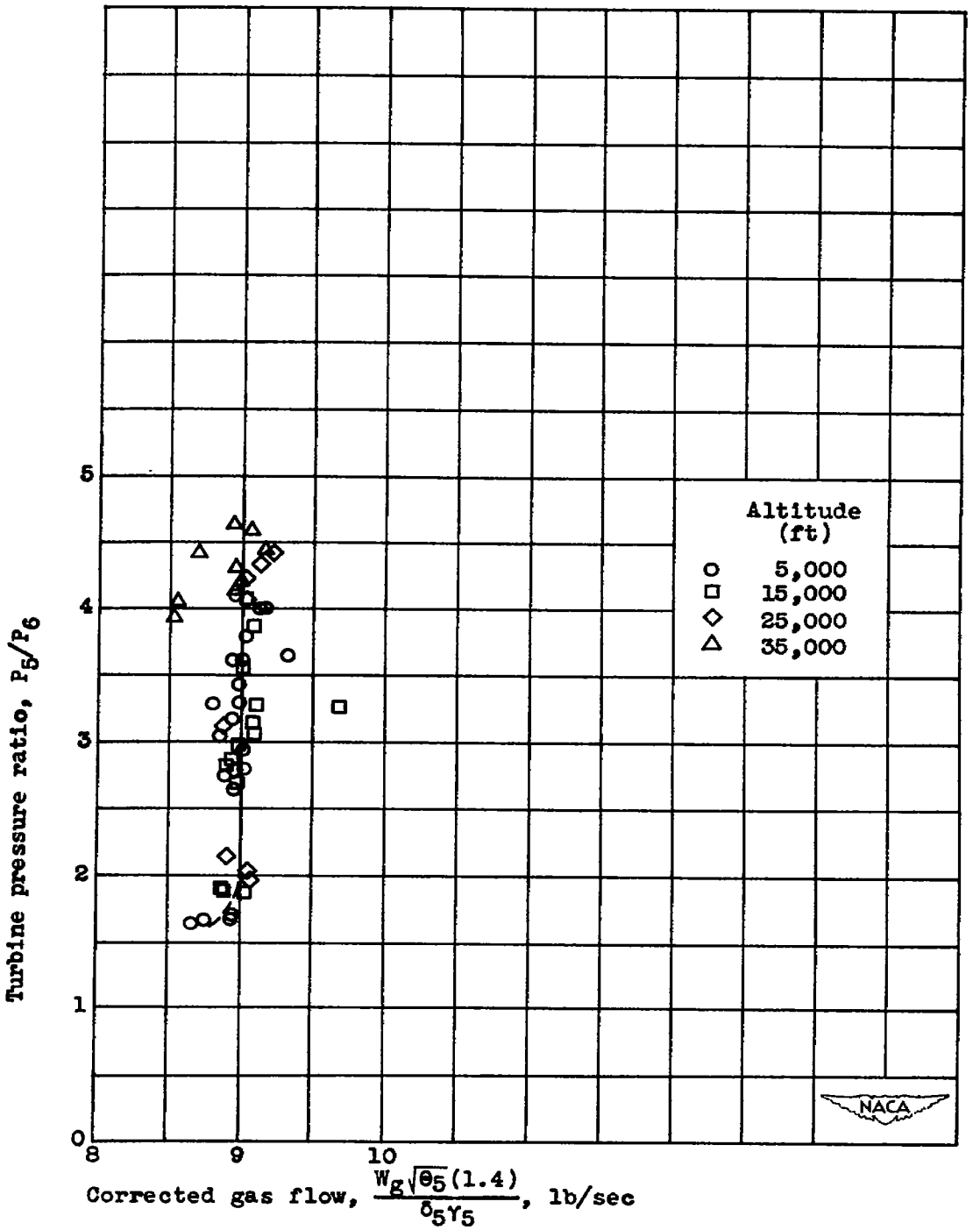

Figure 23. - Variation of turbine pressure ratio with corrected gas flow. Compressor-inlet ram-pressure ratio, 1.00.

NASA Technical Library
3 1176 01435 5409